"FABRICATION OF LDH SUPPORTED HOMOGENEOUS & HETEROGENEOUS BIMETALLIC NANOCOMPOSITES AND IT'S CATALYTIC APPLICATIONS"

A

Thesis submitted

In the partial fulfilment of the requirement for the degree of

MASTERS OF SCIENCE

IN

CHEMISTRY

Submitted by

NIDHI ARORA
(301502023)

Under the supervision of

Dr. SOUMEN BASU

(Associate Professor)

SCHOOL OF CHEMISTRY & BIOCHEMISTRY,

THAPAR UNIVERSITY

PATIALA 147004

2017

SELF DECLARATION

The work embodied in the project entitled "**Fabrication of LDH Supported Homogeneous & Heterogeneous Bimetallic Nanocomposites and Its Catalytic Applications**" has been done by me in the partial fulfilment of requirement for the award of degree of Masters of Science in Chemistry, submitted in the School of Chemistry and Biochemistry, Thapar University, Patiala, is an authentic record of my own carried out under the supervision and guidance of **Dr. Soumen Basu**, Associate Professor, School of Chemistry and Biochemistry, Thapar University, Patiala. All the ideas and references have been duly acknowledged.

Date: 7th August 2017

Place: Patiala

Nidhi Arora

This is to certify the above statement made by student concerned is correct and true to the best of my knowledge.

Dr. SOUMEN BASU

Associate Professor

School of Chemistry and Biochemistry

Thapar University

Patiala

CERTIFICATE

This is to certify that the thesis entitled "**Fabrication of LDH Supported Homogeneous & Heterogeneous Bimetallic Nanocomposites and Its Catalytic Applications**" submitted by **Ms. Nidhi Arora** in the partial fulfilment of the requirements for the degree of Master of Science in Chemistry from Thapar University, Patiala is a bonafied piece of work carried out under the guidance and supervision of **Dr. Soumen Basu**, Associate Professor, School of Chemistry and Biochemistry, Thapar University, Patiala and no part of this project has been submitted for award of any other degree in this or any other university.

NIDHI ARORA

This is to certify the above statement made by student concerned is correct and true to the best of my knowledge.

Dr. SOUMEN BASU

Associate Professor

School of Chemistry and Biochemistry

Thapar University

Patiala

ACKNOWLEDGEMENT

The piece of work would never have been accomplished without the blessings of God and also without the people in my life inspiring, motivating, guiding and accompanying me throughout my dissertation.

I own a deep sense of gratitude to my supervisor ***Dr. Soumen Basu****, Associate Professor, and* ***Dr. Amjad Ali****, Head of Department, School of Chemistry and Biochemistry, Thapar University, Patiala for his keen interest, expert guidance, and motivation during my project work. I am thankful for his valuable suggestions and constructive criticism until the completion of my project. The blessing, help and guidance given by him time to time shall carry me a long way in the journey of life on which I am about to embark.*

I extend my special thanks to the PhD scholars ***Mr. Amit Mishra****,* ***Ms. Akansha Mehta*** ***Ms. Manisha****,* ***Ms. Shagun*** *and my lab-mates* ***Dimple Garg*** *and* ***Shruti Parashar*** *for their immense cooperation, timely help and moral support provided by them during the complete span of my project.*

I would also like to acknowledge ***Nitya Chawla****,* ***Satinder Kaur****,* ***Bhavya Khurana****,* ***Nishant Thakur****,* ***Bimal Garg*** *and* ***Pranshu Puri*** *for their unfailing support, wishes and continuous encouragement for the successful completion of this thesis.*

Words are not enough to express my feelings about my immense gratitude that I owe to my dear parents for their endless love, blessings and moral support throughout my life. Last but not the least I am thankful to all the persons who helped me directly or indirectly during the tenure of my project work.

Nidhi Arora

ABSTRACT

Bimetallic nanoparticles that are made up of two metal elements in a particle exhibit much higher catalytic activity than monometallic ones because of new bi-functional or synergistic effects, so called a ligand and/or an ensemble effect. In this work, a novel homogeneous as well as heterogeneous Au-Ag bimetallic nanocatalyst have been synthesized, supported on layer double hydroxide (LDH) by a simple wet chemical process. The support of LDH has reduced the size as well as capped the bimetallic nanoparticles and hence prevents the agglomeration. The surface morphology and chemical composition of these bimetallic nanoparticles were examined by scanning electron microscopy, transmission electron microscopy, X-ray diffraction, and X-ray photoelectron spectroscopy. It was found that alloyed Au–Ag bimetallic nanoparticles (40-60 nm) are formed. Moreover, catalytic activity for 4-nitrophenol reduction was probed for this as synthesized Au-Ag bimetallic nanoparticles with a variety of compositions. The highest activity was seen for the Au-Ag nanoparticles prepared with Au-Ag ratio at 1:3 and the activity became 10 to 45 times higher than the original monometallic Au or Ag nanoparticles. The rate kinetics was studied for both homogeneous and heterogeneous system on the reduction of 4-nitrophenol and observed that the rate of reduction was greater in case of homogenous catalysts as compared to heterogeneous catalysts. Also, the heterogeneous catalysts were effortlessly recovered and reused (up to 5 cycles) after completion of the reaction.

GRAPHICAL ABSTRACT

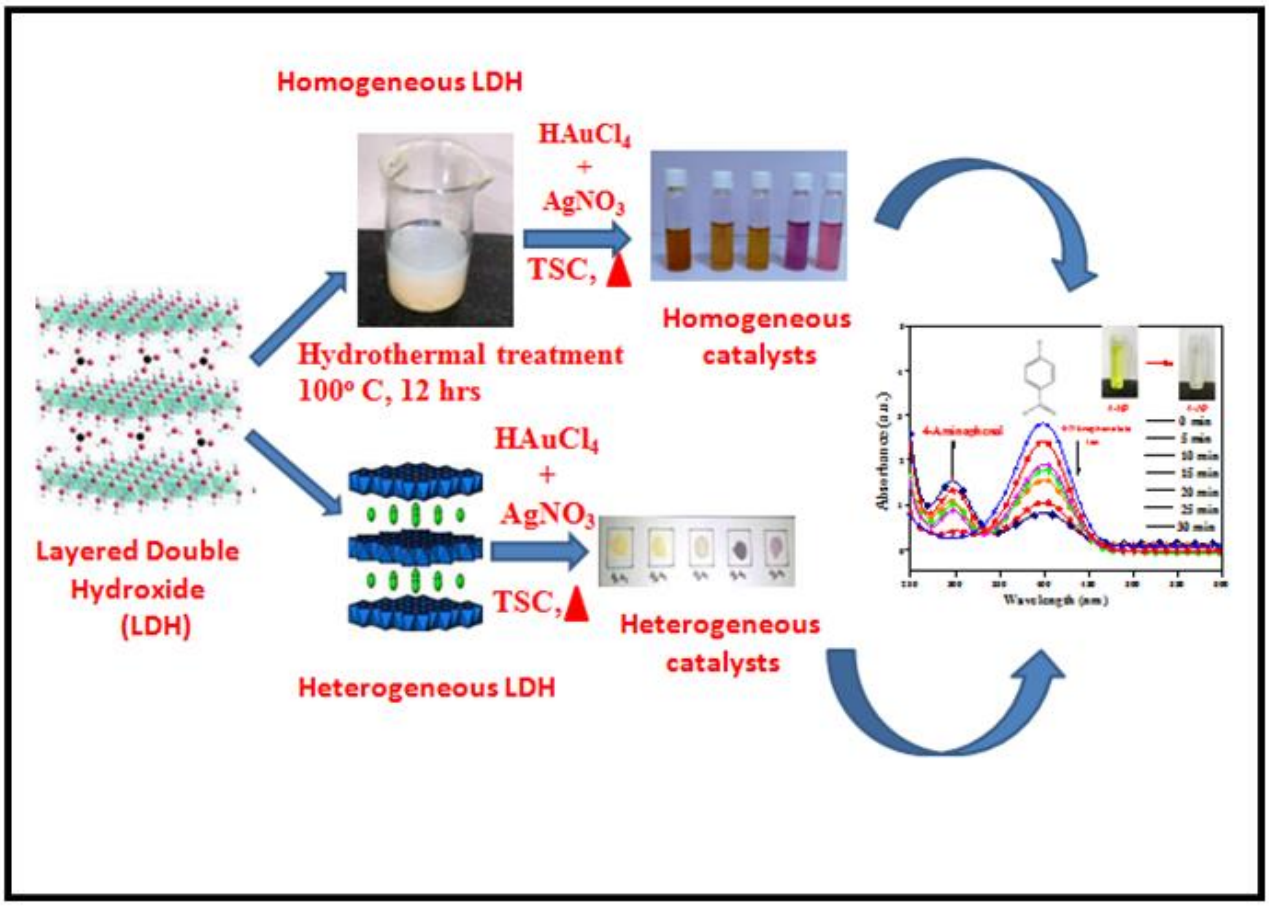

TABLE OF CONTENTS

LIST OF FIGURES AND TABLES

LIST OF TABLES

LIST OF ABBREVATIONS AND SYMBOLS

1.	**BM**	Bimetallics
2.	**BET**	Brunauer-Emmett-Teller
3.	**NP's**	Nanoparticles
4.	**NP**	Nitrophenol
5.	**AP**	Aminophenol
6.	**G**	Gram
7.	**^{o}C**	Degree Celsius
8.	**H**	Hours
9.	**Min**	Minutes
10.	**DLS**	Dynamic light scattering
11.	**λ_{em}**	Emission wavelength
12.	**EDX/EDS**	Energy dispersive X-ray spectroscopy
13.	**λ_{ex}**	Excitation wavelength
14.	**SPR**	Surface Plasmon Resonance
15.	**AuNP's**	Gold nanoparticles
16.	>	Greater than
17.	**@**	Supported
18.	<	Less than
19.	**Nm**	Nanoparticles
20.	**λ_{max}**	Maximum wavelength
21.	**LDH**	Layered Double Hydroxide
22.	**SERS**	Surface Enhance Raman Scattering
23.	**Ag NP's**	Silver nanoparticles
24.	**µL**	Micro litre
25.	**µM**	Micro molar
26.	**DRS**	Diffuse Reflectance Spectrophotometer
27.	**MW**	Molecular Weight
28.	ζ	Zeta Potential
29.	**%**	Percent

30.	**SEM**	Scanning electron microscope
31.	**TEM**	Transmission electron microscope
32.	**UV-Vis**	Ultraviolet-Visible
33.	**W**	Watt
34.	**XRD**	X-ray Diffractometer
35.	**XPS**	X-ray photoelectron spectroscopy

CHAPTER 1: INTRODUCTION

1.1 Catalysts

Catalyst is a material which alters the rate of a chemical reaction. These materials are not consumed in the course of reaction and stay the same. Catalyst assists a chemical reaction by lowering the activation energy of the reactants to produce desired products. In general, catalytic action can be seen as a chemical reaction between the catalyst and the reactant, that form intermediates which react more readily with each other or with other reactant, to form the required product. During the course of reaction between the intermediates and reactants, catalyst is regenerated. The modes of reactions between the catalysts and the reactants vary widely. The typical examples of these reactions include the acid–base reactions, redox reactions, formation of coordination complexes, and formation of free radicals. In case of solid catalysts, the mechanism of reaction is strongly influenced by surface enhanced properties and electronic/crystal structures.

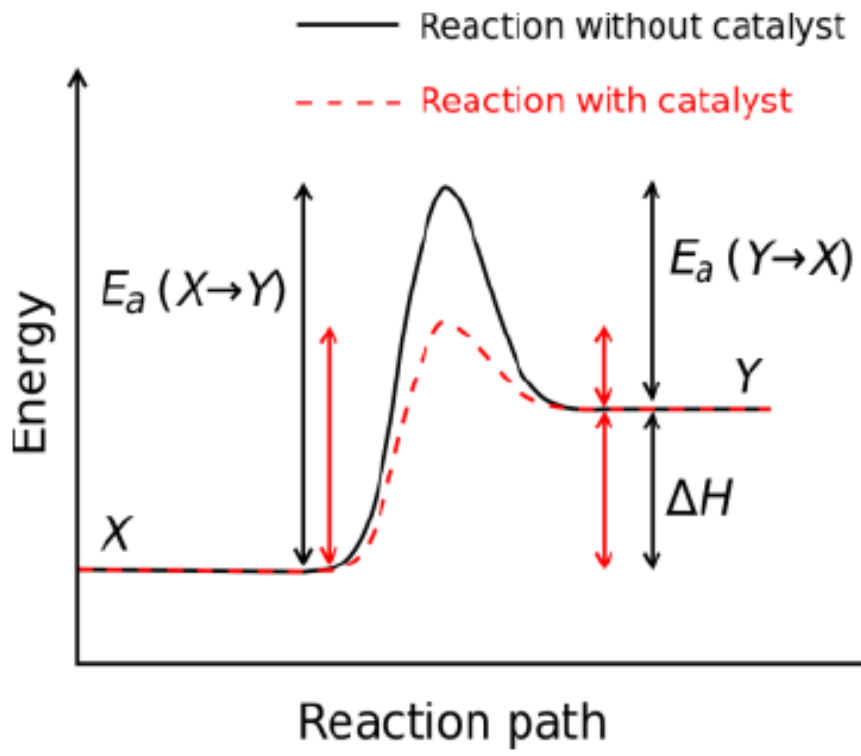

Fig. 1: **Schematic representation energy of activation in a chemical reaction with and without a catalyst.**

The catalysts are majorly divided into two categories:

- Homogeneous catalysts
- Heterogeneous catalysts

1.1.1 Heterogeneous Catalysts

Heterogeneous catalysis refers to the form of catalysis where both the catalyst and reactants are in the different phase. Catalyst is normally in solid phase and it assists reaction by temporary bonding atoms to its surface, which allows their internal bonds to break more rapidly. Such catalysts are widely used in industry. The example includes the use of finely divided platinum to catalyze the reaction of carbon monoxide with oxygen to form carbon dioxide.

1.1.2 Homogeneous Catalysts

Homogeneous catalysis refers to a form of catalysis in which both the catalyst and reactants are in same phase. In most of the industry processes, homogenous catalysts are replaced by heterogeneous due to their ease of separation, regeneration and reusability. Enzymes are the perfect example of homogeneous catalyst. Homogeneous catalysts are known for their high selectivity and conversion whereas heterogeneous catalysts are known for their ease of separation, regeneration and reusability.

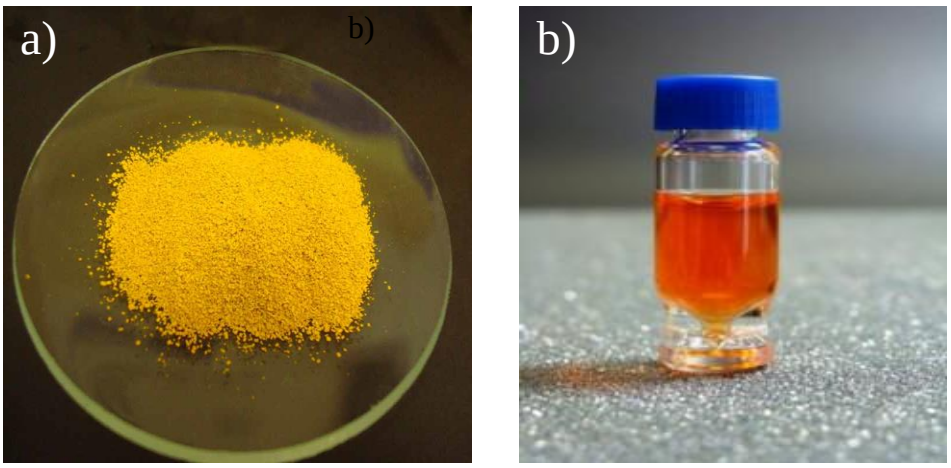

Fig. 2: The figure contains samples showing a) heterogeneous catalyst and b) homogeneous catalyst.

1.1.3 Why Catalysts?

In recent years, environmentally benign chemical synthesis and methodologies have received much attention from scientists, because they are essential for conservation of global ecosystem. In the present era, most of the chemical industry processes are dependent on catalyst as it is well said “they are the backbone of chemical industry.” Most of the chemical processes in food, pharmaceuticals, automobiles, fertilizers and petrochemical industries mainly depend on catalyst. Hence the design and development for catalyst for the conversion of raw materials into value added chemicals has become a major area of research in industry and academia. Considering the catalytic viewpoint, it is essential to decrease the size of bulk material particle from several micrometres to nanometres so that there is an increase in its surface area.

1.1.4 How Catalyst Works?

The catalyst works by providing an alternative surface which enables a different pathway for the chemical reaction to occur. The particle which has to react attaches itself on the surface of catalyst and collides more often with each other. Most of the collisions result in the reaction because the catalyst provides a different route that has lower activation energy. A catalyst is mostly used as a fine powder because it has a bigger surface area available for the reaction to take place. This has been illustrated in the figure below.

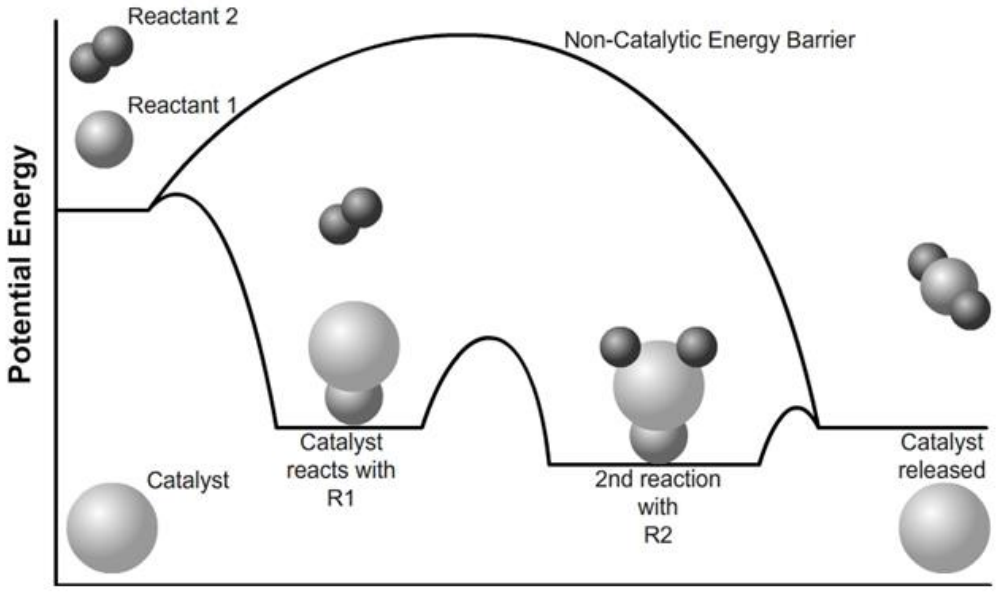

Fig. 3: The mechanism followed by the catalyst during course of reaction.

1.2 Bimetallic Compounds

Bimetallic compounds with a nano-size (1-100 nm) have been the subject of significant scientific interest as efficient catalyst with vastly improved activity and selectivity compared to their monometallic counterparts [1-4]. Among various metals, the coinage metals (Cu, Ag and Au) nanoparticles (NP's) have drawn much attention due to their unique optical, electronic and catalytic properties [5].Au and Ag NP's have attracted significant attention because of their unique physical and chemical properties, and their applications in photonics [6], catalysis [7], information storage [8], chemical and biological sensing [9, 10] and surface enhance Raman scattering (SERS) [11]. Au NP's have been extensively studied because of their high resistance to oxidation, facile synthesis, surface plasmon effect (SPR) and have much catalytic application such as hydrogenation of nitro aromatic compound and carbon-carbon bond formation [12].

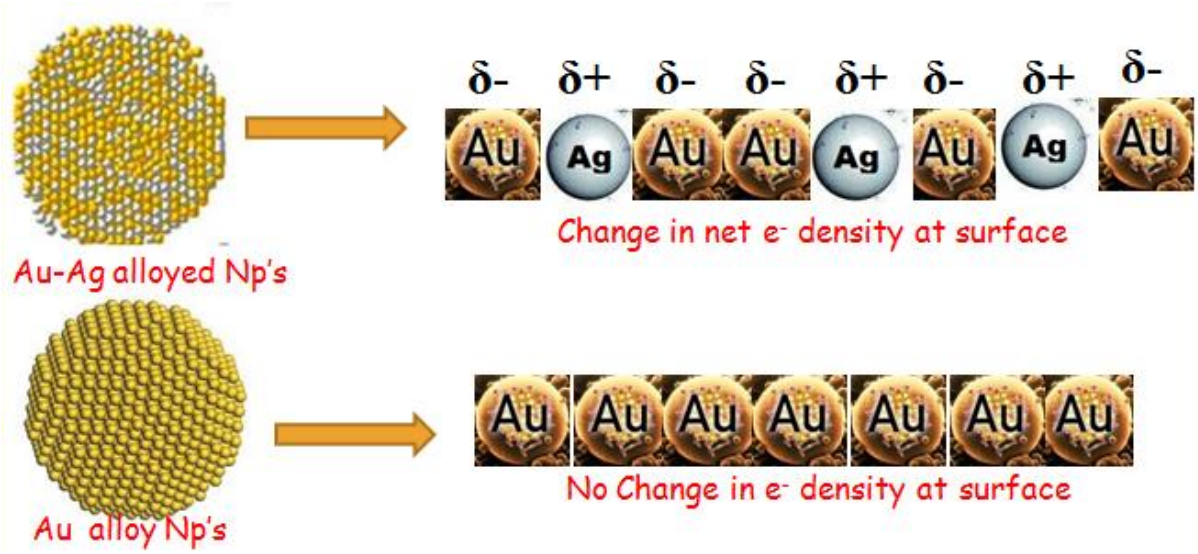

Fig 4: Pictorial representation for alteration of charge

1.2.1 Advantage of Bimetallic Over Monometallic Compounds

The incorporation of another metal Ag to Au results in active site isolation which leads to alteration of electronic structure of Au via chemical bonding and due to this high catalytic activity was seen [13]. The physiochemical properties of plasmonic metal NP's improve considerably by introduction of second metal [5, 13]. In the previous years, much progress has been made in the synthesis of bimetallic NP's following a variety of synthetic strategies, including co-reduction, galvanic replacement, thermal decomposition, photochemical, successive reduction, and electrochemical deposition methods**.** They can adopt either core-shell or alloy structures depending upon the synthetic approach followed.

The site isolation of the active metal in these structures, affords geometric and electronic changes directed toward noticeable enhancement in activity, selectivity, and stability during catalysis [14].The source of the synergistic effect that exists among two metals is still not fully understood but it is thought to originate due to formation of alloy that leads to electronic (ligand) and geometric (ensemble) effects resulting in enhanced catalytic activity in the reduction reaction. The electronic and geometric modifications can be accomplished by altering the bimetallic structure, surface composition, particle size, and its distribution, all of which are dependent on the procedures followed for preparation and post activation treatments [15].

1.2.2 Influence of Size

Literature reveals that a particle of size 30 nm has 5% of its atoms on the surface, 10 nm has 20%, and 20 nm has 50% exposed surface atoms which can efficiently participate in a chemical reaction as shown in Scheme below.

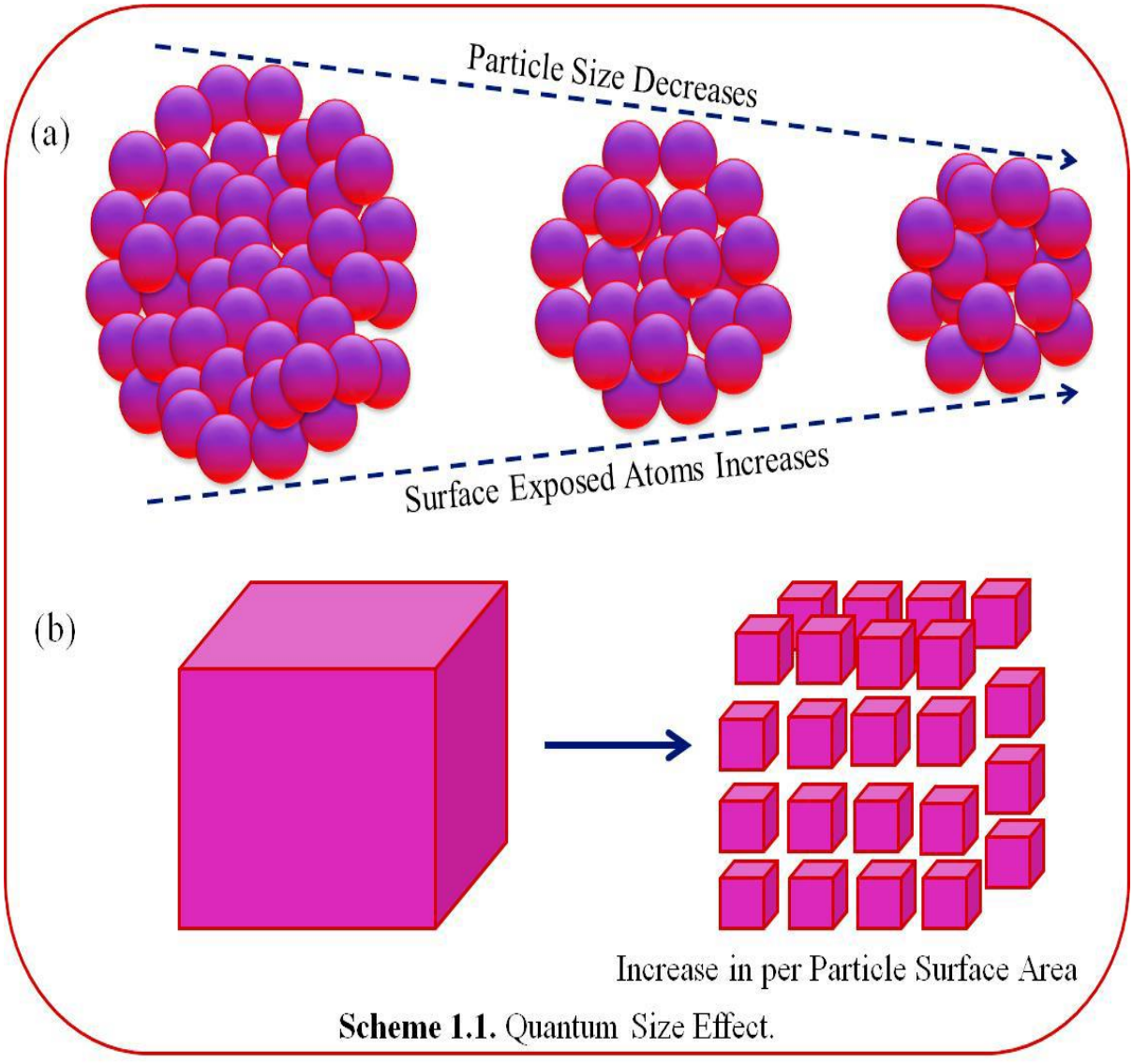

Scheme 1.1. Quantum Size Effect.

It shows that when a bulk material is subdivided into individual NP's; the total volume remains constant, but the surface area increase and hence, intends to show a profound effect on catalytic performances. Therefore, the smaller particles are found to be more active because of the large number of surface active atoms available for catalysis. The catalytic activity of metal NP's was reported to increase with decreasing particle size in case of nitro-aromatic reduction.

1.3 Layered Double Hydroxide (LDH)

The NP's with such minute size tends to aggregate and hence reduce their surface area; as a result of this agglomeration their catalytic activity may get significantly deteriorate. These NP's could be effectively stabilized by the appropriate supports that hold their high surface area and activity of catalyst [16]. Among these support materials, Layered double hydroxide (LDH) is one of the most widely used supports and is gardening importance due to its intercalation properties. The support of LDH will further reduce the size of NP's and hence prevent the agglomeration of NP's.

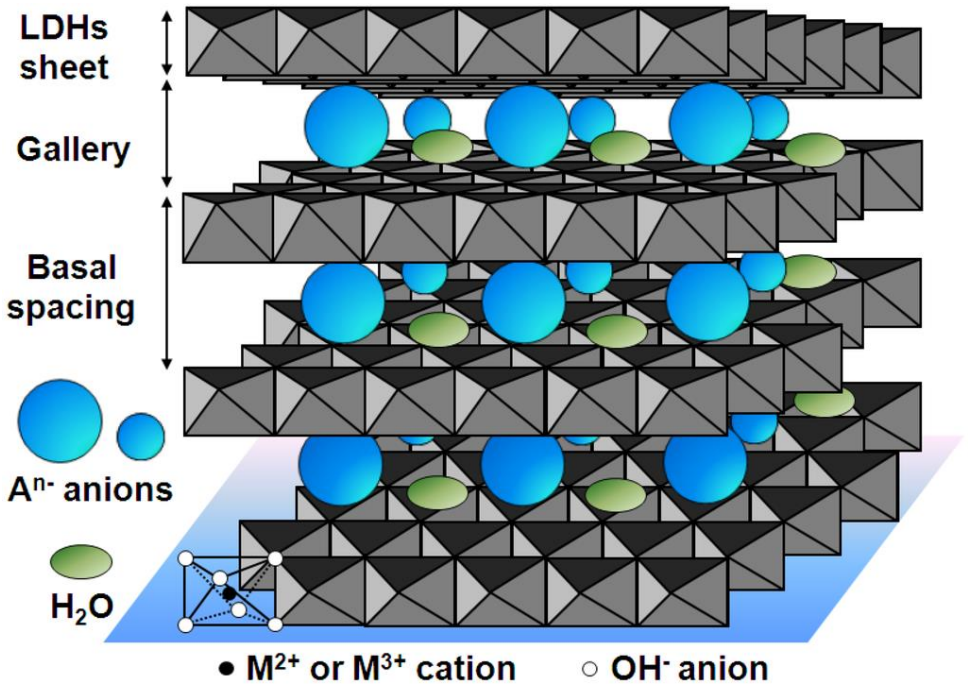

Fig. 5: A pictorial representation of Layered Double Hydroxide.

LDH is composed of cationic brucite-like layers $[M^{2+}_{1-x} M^{3+}_{x} (OH)_2]_x^+$ in which some of M^{2+} is replaced by M^{3+} and the anions and sometimes the water molecules are also present in between the brucite-like layers that balances the positive charge [17].The NP's are supported on this LDH to increase its chemical reactivity. The homogeneous catalyst is supported on homogeneous LDH and heterogeneous catalyst on heterogeneous LDH.

1.4 Why Nitro- Phenol Reduction?

To have a concrete knowledge about size-specific catalysis, some reaction is chosen and performed. Here, the model reaction selected is reduction of 4-nitrophenol (4-NP) to 4-aminophenol (4-AP), because making of many analgesic and antipyretic drugs, such as paracetamol, etc, needs 4-AP as a potent intermediate [18]. It is also used enormously as a developer in photographic plates, inhibitor of corrosion, anticorrosion-lubricant, and hair-dyeing agent [19, 20]. Water pollution by phenol and phenolic compounds is of great concern and nitro-phenols are the most intractable pollutants that occur in industrial wastewater. More particularly, nitro-phenol and its derivates result from the production processes of pesticides, insecticides and synthetic dyes that contribute immensely in increasing the pollution [21]. So, this study becomes much more important from the environmental point of view. There is a great demand of aromatic amino compounds industrially, so this reaction is important from academic as well as industrial point of view. Thus, being a common antecedent material for 4-AP, a newer and cheaper method for hydrogenation of 4-NP is always in demand.

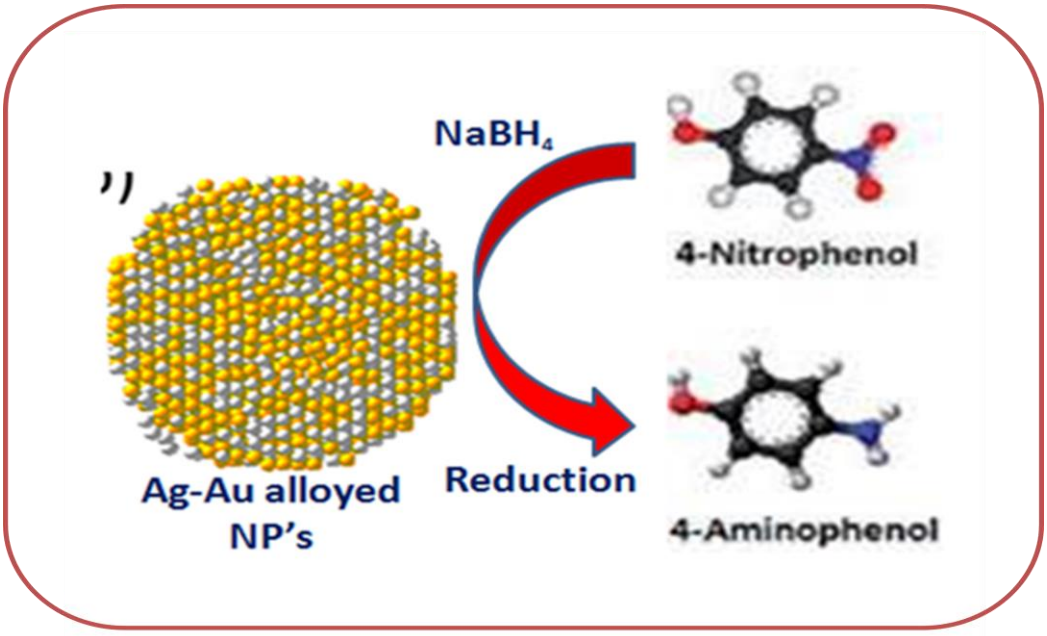

Fig. 6: Schematic representation of conversion of nitro-phenol to aminophenol.

The conventional methods for hydrogenation of 4-NP involves iron/ acid as a reducing agent which has certain limitations such as metal oxide in huge amount are produced as sludge of these reactions. In current years, the reduction of 4-NP to 4-AP by $NaBH_4$ in aqueous solution is becoming important because it can be monitored easily with high precision by UV-Vis spectroscopy. This is due to the fact that 4-NP has a strong absorption at 400 nm and the decay of this peak can be measure precisely as the function of time [22].

In the present study, alloyed Au-Ag bimetallic NP's impregnated on LDH were synthesized to study the comparative reduction of NP's relative to their monometallic NP's using $NaBH_4$ as a reducing agent. Also we have tried to probe the differences in catalytic activity of homogeneous and heterogeneous catalyst. This work has allowed us to draw clear conclusions regarding the effect of concentration of reactant, catalyst, reducing agent on the rate constant of the reaction.

1.5 Methodology

The synthesis of NP's basically follows two main approaches. These include:

- Top-down approach
- Bottom-up approach

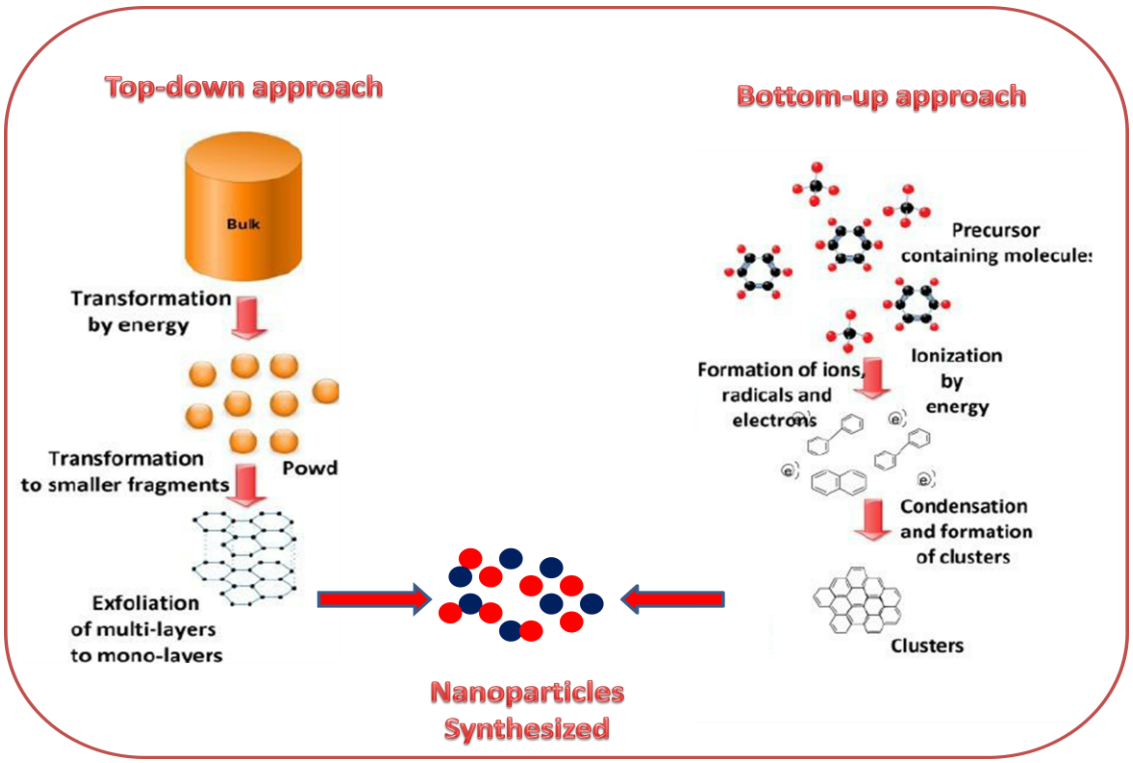

Fig. 7: The figure depicts the two famous approaches for the formation of nanoparticles.

1.5.1 Top-Down Approach

This top down approach to synthesize NP's include cutting down of the bulk material to get the desired NP's. These approaches use larger (macroscopic) initial structures, which can be externally-controlled in the processing of nanostructures. Typical examples are etching through the mask, ball milling, and application of severe plastic deformation.

1.5.2 Bottom-Up Approach

These approaches include the miniaturization of materials components (up to atomic level) with further self-assembly process leading to the formation. During self-assembly the physical forces operating at nanoscale are used to combine basic units into larger stable structures. Typical examples are quantum dot formation during epitaxial growth and formation of nanoparticles from colloidal dispersion.

1.6 Catalytic Reaction

The 4-NP reduction using $NaBH_4$ was studied to probe the catalytic activity of both the heterogeneous and homogenous catalysts. The reaction was studied in a quartz cuvette. 2.77 mL water was taken with 30 μL (10^{-2} M) of 4-NP and 200 μL of freshly prepared $NaBH_4$ (10^{-2} M). Thus the final concentration of 4-NPwas reached to 10^{-4} M and that of $NaBH_4$ became 6.67 x 10^{-3} M. At this time, the 4-NP was transformed into 4-nitrophenolate anion. To the mixture 20 μL/1 mg of catalyst is added and immediately after addition the spectra was taken and a noticeable increase in peak of 4-AP was seen at ~300 nm. A gradual change in the colour of solution from yellow to colourless was observed in the reaction. In a same pattern, the study was conceded out for different catalyst by changing ratio of Au and Ag.

1.7 Catalyst Characterisation

Various instrumental techniques have been used to characterize the NP's to get an plan about their size, shape, morphology, surface area, physicochemical properties, etc. which are described below.

1.7.1 UV-Vis Spectrophotometer

UV-Vis spectroscopy is a technique used to enumerate the light that is absorbed and scattered by the sample. Coinage metal NP's possess the optical properties that depend on its morphology, refractive index and the concentration that makes it an important method for the identification and characterization of these nanomaterials. The NP's strongly interact with a

specific wavelength of light which results in the promotion of an e- to a higher energy level and hence, an absorption peak. The analysis was done by taking ~2.5 mL colloidal NP solution in a quartz cuvette within the range of 190-700 nm.

1.7.2 Diffuse Reflectance Spectrophotometer (DRS)

Diffuse reflectance spectrophotometer (DRS) was used to determine the reflectance/absorption of as prepared monometallic and alloy Ag-Au@LDH NP's in the UV-Vis region. The sample (2-5 mg) was taken in a vial and the light source probe was placed over the sample to record its absorbance/ reflectance spectra by using $BaSO_4$ as a reference.

1.7.3 Dynamic Light Scattering (DLS)

Dynamic light scattering (DLS) is a technique used to determine the hydrodynamic size of NP's dissolved in suspension or solution. The particle size distribution was determined by using a Brookhaven 90 plus Particle Size Analyzer by taking 2.5-3 mL of dispersed NP's solution in a cuvette. The Brownian motion of small particles in suspension causes the laser light to be scattered at different intensities. By measuring the time scale of these light intensity fluctuations, DLS can yield information regarding the average size or size distribution of particles in solution.

1.7.4 Zeta Potential Measurement

When the NP's are suspended in an aqueous medium, the adsorption or ionization of ions takes place on the NP's surface, which leads to the formation of an electrical double layer resulting in the development of net charge, called zeta potential (ζ). Therefore, zeta potential is an important tool for understanding the state of NP's surface and also predicts the long term stability of the NP's. The measurements were carried out at 25 ºC using a cuvette comprising a palladium electrode mounted on a machine support immersed in 1.5-2 mL of NP solution.. Zeta potential of the catalyst was analysed using Zetasizer Nano (Malvern-ZEN-1690).

1.7.5 Energy Dispersive X-Ray Spectroscopy (EDS)

Energy Dispersive X-ray (EDS) Spectroscopy was used for the elemental analysis or chemical composition of the selected points or areas of the sample qualitatively and semi quantitatively. This technique was used as an attachment on scanning electron microscopy (SEM) or transmission electron microscopy (TEM) and utilizes the high-energy e- that are ejected by an elastic collision of an incident e- with sample's atom nucleus and are referred to

as back scattered e-. The yield of backscattered is in proportional to the atomic number of an element and therefore, the sample composition, elements and compounds, and their relative ratios in the area of one micrometre in diameter are determined using this technique. This EDX analysis was carried on JEOL JSM-6510LB.

1.7.6 Transmission Electron Microscopy (TEM)

It is used to identify finest structural details of individual particles and their statistical size and shape distribution in the samples. In this technique, a beam of e- is transmitted through the sample and due to this interaction an image is formed, then magnified and focused onto an imaging device. TEM images of the catalysts were obtained using a Technai-12, FEI Netherlands at an accelerating voltage of 120 kV. The specimens were made by dispersing the samples in methanol using an ultrasonic bath and evaporating a drop of resultant suspension onto the carbon-coated copper grid.

1.7.7 X-Ray Photoelectron Spectroscopy (XPS)

XPS was used to study the chemical composition and oxidation state of catalyst surfaces. The XPS spectra of the catalysts were measured using XPS spectrometer (KRATOS Axis 165, Shimadzu, UK) with Mg K_α radiation 1253.6 eV at 75 W. The gold 4f and silver 3d core-level spectra were recorded and the corresponding binding energies referenced to the C 1s line at 284.6 eV (accuracy within 0.2 eV). The background pressure during the data acquisition was kept below 10^{-9} torr.

1.7.8 X-Ray Diffraction (XRD)

The chemical composition of the catalyst was investigated using X-Ray diffraction technique at a scanning rate of 2 °/min from $2\theta = 5°$ to 80°with Co Kα radiation on a Bruker Diffractometer

1.7.9 Nitrogen Sorption Analysis

Nitrogen adsorption and desorption isotherms at 77 K were performed to calculate the surface area of the catalysts after pre-treatment at 523 K for about 2 h by using BEL-miniII, Microtrac Corp. Pvt. Ltd. Pore size distribution were calculated though BJH model from N_2 desorption isotherms.

CHAPTER-2: LITERATURE REVIEW

The use of catalyst is becoming increasingly popular because of its ease with which it increases the rate of reaction. Earlier only a single metal were used as catalyst to carry the reaction. With further advancements, it was found that the addition of another metal causes alteration of charge on the surface which greatly increases the rate of reaction and hence they become more popular. The addition of support to NP's prevented its agglomeration and reduced its size considerably. The further reduction in size lead to increase in the surface area due to which more surface was available for the reaction to occur. So, the addition of support was found to be helpful and is becoming increasingly popular now-a-days.

BM NP's with controlled morphologies and composition has exhibited superior properties and broader applications in comparison to their monometallic counterparts. In recent years, the research towards the variety of BM NP's with diverse combinations of metals and morphologies has been developing and reported. Despite this fast progress in the exploration of BM NP's, challenges still remain in the following direction-

The synergistic electronic effect at the interface of the two metals in BM NP's enhances its catalytic efficacy. As a result, they have the potential that exhibit higher catalytic activity and other functionalities by continual tuning through the different combinations of metal elements and the composition of the constituents. Therefore, how the nature of metals and shape affect the reactivity and selectivity during the catalytic process is an emerging field of research.

The studies for alloyed Au-Ag bimetallic NP's supported by LDH was taken into consideration because many reports are found which use merely Au or Ag monometallic NP's to reduce the nitro-phenol compounds, but very few studies are reported for Au-Ag alloy NP's supported on LDH. In one of the reports, Jianping *et al*. has reported the synthesis of graphene oxide decorated Au–Ag bimetallic alloy by a two-step method which exhibits superior catalytic performance for the reduction of 4-nitrophenol (4-NP) [23]. Pozun *et al*. reported the 4-NP reduction using bimetallic dendrimer encapsulated nanoparticles (Pt/Cu, Pd/Cu, Pd/Au and Au/Cu)[24]. Also Zhang *et al*. systematically studied the reduction of 4-NP by using Au decorated ceria nanotubes[25]. But there is no report for the synthesis of homogeneous/heterogeneous Au–Ag bimetallic NP's on LDH support. Also there are only

few reports available for the comparison of bimetallic NP's in heterogeneous and homogeneous catalysis reaction.

Table 1: Comparison table of the previous studies done.

Catalyst	Concentration of NP	Catalyst loading	Catalytic efficiency/rate constant	Reaction time	Reference
AgNP's	10^{-4} M	3.5377 × 10^{-5} g L^{-1}	17.04 ×10^{-3} s^{-1}	500 seconds	[26]
Au/SiO2	0.005 M	5 mg	98 %	20 minutes	[22]
Au,Ag, Pd	50 µM	8 ml, 5 µM	0.0027 min^{-1} (Au), 0.0558 min^{-1} (Ag),0.9993 min^{-1}(Pd)	200 seconds	[27]
PGMA@PAH@Au NP's	0.1 mM	5.4241 10^{-12} moles	1.4 ×10^{4} s^{-1}	82 seconds	[28]
Platinum nanoparticles stabilized by guar gum	1 mM	5 mM	7×10^{-3} s^{-1}	300 seconds	[29]

In comparison with other published works, the as synthesized Au-Ag bimetallic alloy NP's supported on LDH showed a high rate for conversion of 4-NP to 4-AP (Table 1). The origin of the intrinsic activity is from the intimate interaction between Au and Ag after formation of Au-Ag alloy NP's. Therefore, it could be considered that as synthesized Au-Ag bimetallic NP's (homogeneous and heterogeneous) could be employed as alternative catalysts for the conversion of 4-NP to 4-AP at room temperature.

Keeping in view the above points, the following objectives have been designed:

(i) Preparation of bimetallic alloys of coinage metals (Au and Ag).

(ii) Optimization of optical properties, structural and morphological parameters (i.e., zeta potential, and particle size distribution as a function of nature of metal.

(iii) Study of the effect of catalyst on the reduction of nitro-phenols.

(iv) Study the kinetics of the reduction reaction.

The motivation for the present work is to try to combine two metals forming an alloy and further supporting it to enhance its catalytic activity. The wet chemical synthesis approach of co-reduction was followed.

.

Thus, in this thesis the next work after the synthesis of various homogeneous and heterogeneous catalysts was to see its activity for the reduction of 4-NP.Our work aims to study the effect of catalyst on the reduction, the variation of reducing agent and the concentration of reactant.

CHAPTER 3: MATERIALS& METHODOLOGY

This chapter deals with the materials and methodology used during the research work done in the lab which includes chemicals and various instruments used such as BET, UV-VIS etc.

3.1 Materials Used

3.1.1 Apparatus

Beakers (50ml and 250 ml), micro pipette, measuring cylinder, filter paper, glass rod, magnetic beads, reagent bottles ,Petri plates, Elisa plate, tips, falcon tubes, spatula, crucible and magnetic stirrer for the preparation solution.

3.1.2 Reagents and Chemicals Used

All the chemicals used were commercially certified reagents and used without further purifications. Aurochloric acid ($HAuCl_4.3H_2O$), silver nitrate ($AgNO_3$), sodium borohydride ($NaBH_4$) and trisodium citrate ($Na_3C_6H_5O_7$) were obtained from Loba Chemie, India. Magnesium chloride hexahydrate ($MgCl_2.6H_2O$), aluminium chloride anhydrous ($AlCl_3$) and 4-nitrophenol were obtained from Spectrochem Chemicals.

3.2 Co-Precipitation Method

3.2.1 Preparation of Homogeneous/ Heterogeneous LDH

The homogeneous LDH was synthesized by co-precipitation method and then was treated hydrothermally at 100° C. To prepare LDH, $MgCl_2.6H_2O$ (30 mmol) and $AlCl_3$ (10 mmol) were added together in 100 mL water resulting in a mixed salt solution. This mixed salt solution was quickly added to 400 mL of NaOH solution (0.15 M) with vigorous stirring for 10-30 min. The LDH so formed was centrifuged and the slurry obtained was washed with deionised water. This aqueous suspension was then transferred into a stainless steel autoclave with a Teflon lining. The autoclave was then placed in a preheated oven followed by hydrothermal treatment at 100° C for 12 h. In case of heterogeneous LDH the slurry so obtained was dried at 80° C for 10 h and a solid powder LDH is obtained.

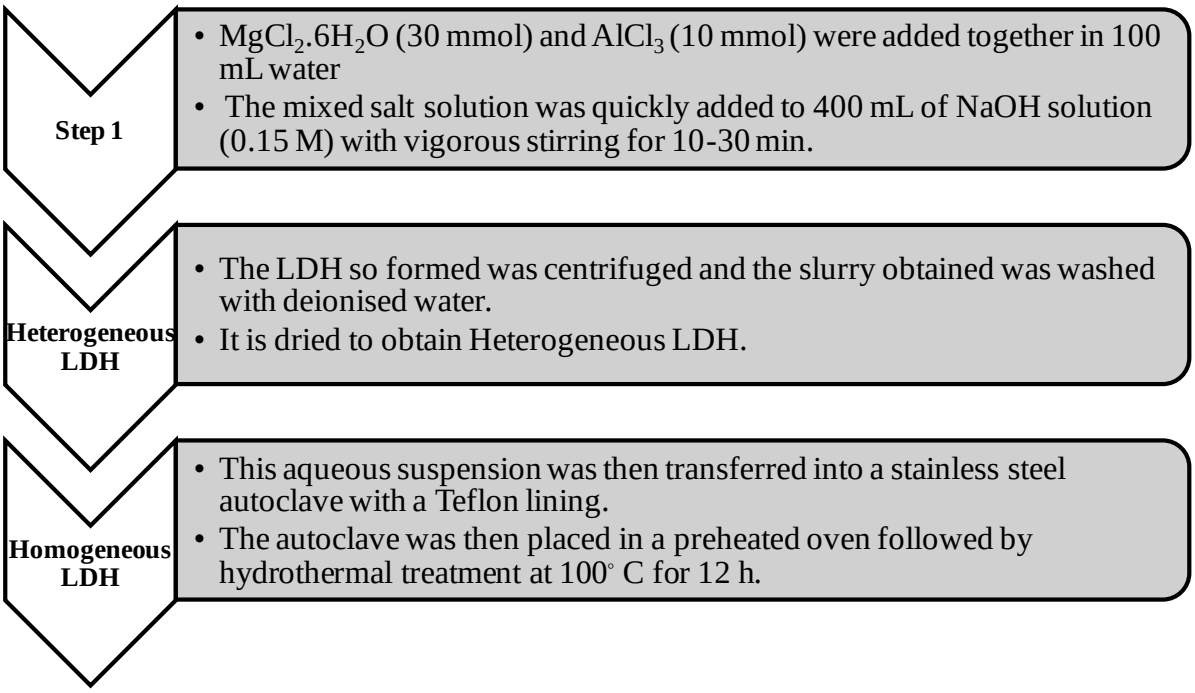

Fig. 8: The flow chart describing the steps involved in the formation of LDH.

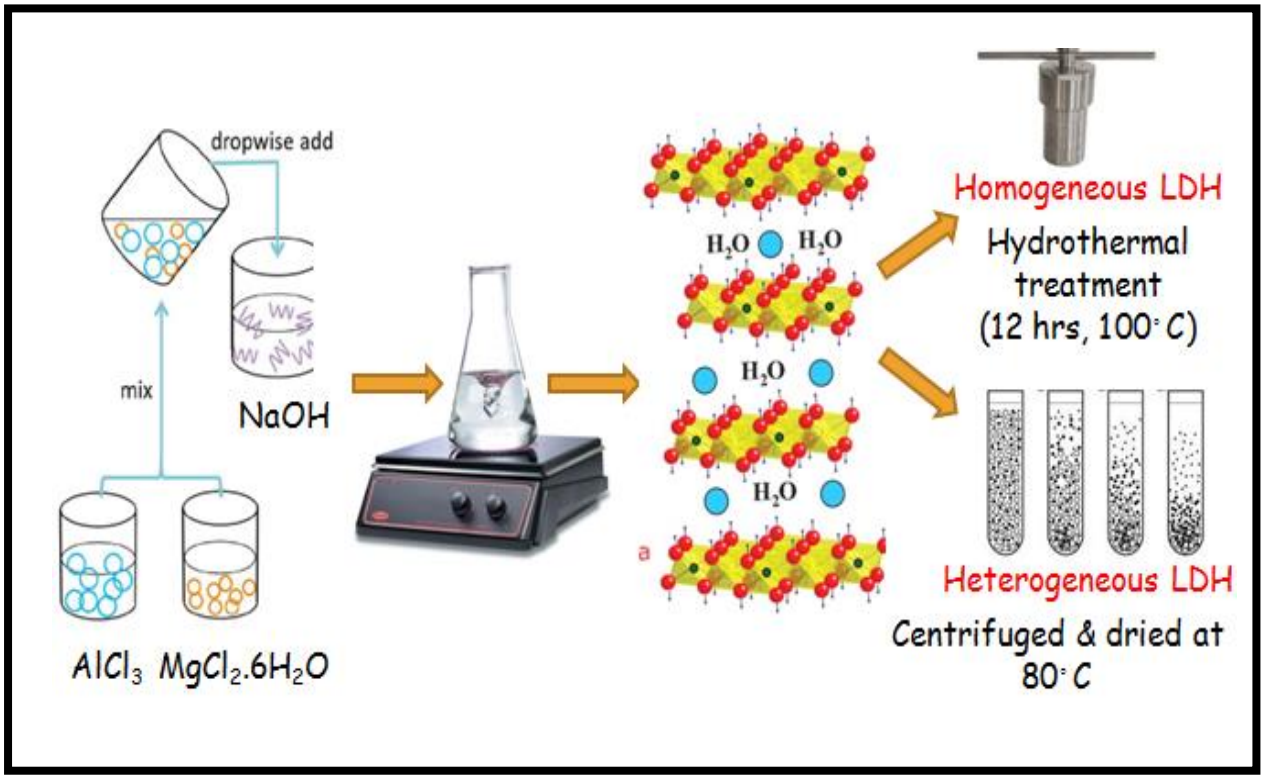

Fig 9: Diagram representing the formation of LDH.

3.3 Co-Reduction

This is a relatively simple method that involves the simultaneous reduction of the metal ions in their atomic form in the presence of suitable stabilizer giving rise to alloy BM NP's as shown in Fig. For example, BM Au-Ag alloy NP's were prepared by the co-reduction of $Au^{3+}$and Ag^{+} metals in the presence of sodium citrate.

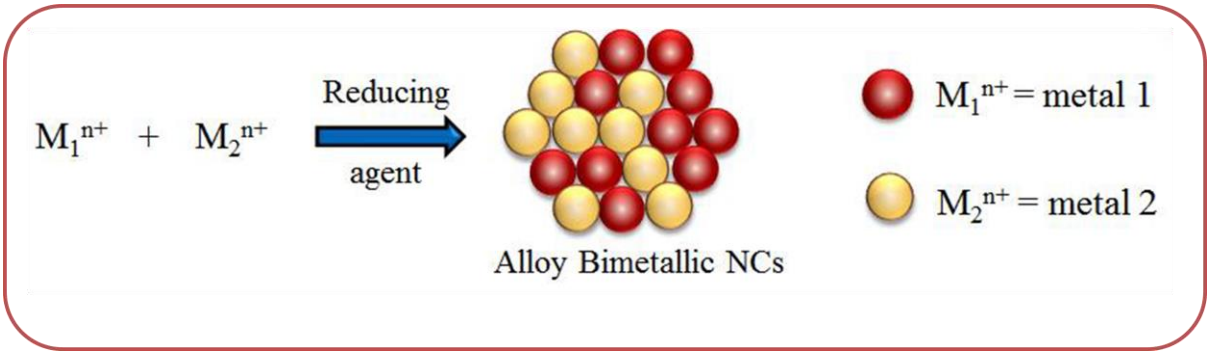

Fig. 10: Schematic representation showing the formation of Alloy Bimetallic nanocomposites via co-reduction method.

3.3.1 Preparation of Homogeneous Au-Ag@LDH NP's

The homogeneous Au-Ag bimetallic NP's supported by LDH were prepared by mixing 5 mL of as-prepared homogenous LDH solution in 50 mL of water with varying amount of $HAuCl_4$ (10^{-2} M) and $AgNO_3$ (10^{-2} M) solution. The mixture was stirred for 12 h. After 12 h, trisodium citrate was added directly to the solution and was heated at 100° C for 4-5 h. The colour of the solution changed which confirm the formation of bimetallic NP's. The detailed amount of salt solution with the molar ratio of Au: Ag is given in Table-2.

3.3.2 Preparation of Heterogeneous Au-Ag@LDH NP's

The heterogeneous Au-Ag bimetallic NP's supported by LDH were prepared by mixing 1 g of as prepared heterogeneous LDH in 50 mL water with varying amount of $AgNO_3$ (10^{-2} M) and $HAuCl_4$ (10^{-2} M). The mixture was stirred vigorously for 12 h. After the vigorous stirring, trisodium citrate was added directly to the solution and the solution was heated at 100° C for 4-5 h. When the colour of the solution is changed, the catalyst is centrifuged, washed with deionised water and dried at 80° C for 10 h. The detail amount of salt solution with the molar ratio of Au: Ag is given in Table-2.

Table 2: Summary of synthesis of various homogeneous and heterogeneous catalysts.

Sample Name	Molar ratio of Ag:Au	Type	LDH (ml/mg)	Volume of $HAuCl_4$ (10^{-2} M) (µL)	Volume of $AgNO_3$ (10^{-2} M) (µL)	Amount of Trisodium Citrate added(mg)
Ag_1Au_1	1:1	Homogeneous	5 ml	0.75	0.75	10
Ag_1Au_3	1:3	Homogeneous	5 ml	2.25	0.75	40
Ag_3Au_1	3:1	Homogeneous	5 ml	0.75	2.25	40
Ag_1Au_5	1:5	Homogeneous	5 ml	3.75	0.75	60
Ag_5Au_1	5:1	Homogeneous	5 ml	0.75	3.75	60
Ag	1	Homogeneous	5 ml	-	1.5	10
Au	1	Homogeneous	5 ml	1.5	-	10
Ag_1Au_1	1:1	Heterogeneous	1 gm	0.75	0.75	10
Ag_1Au_3	1:3	Heterogeneous	1 gm	2.25	0.75	40
Ag_3Au_1	3:1	Heterogeneous	1 gm	0.75	2.25	40
Ag_1Au_5	1:5	Heterogeneous	1 gm	3.75	0.75	60
Ag_5Au_1	5:1	Heterogeneous	1 gm	0.75	3.75	60
Ag	1	Heterogeneous	1 gm	-	1.5	10
Au	1	Heterogeneous	1 gm	1.5	-	10

Graphical representation for the synthesis of catalysts.

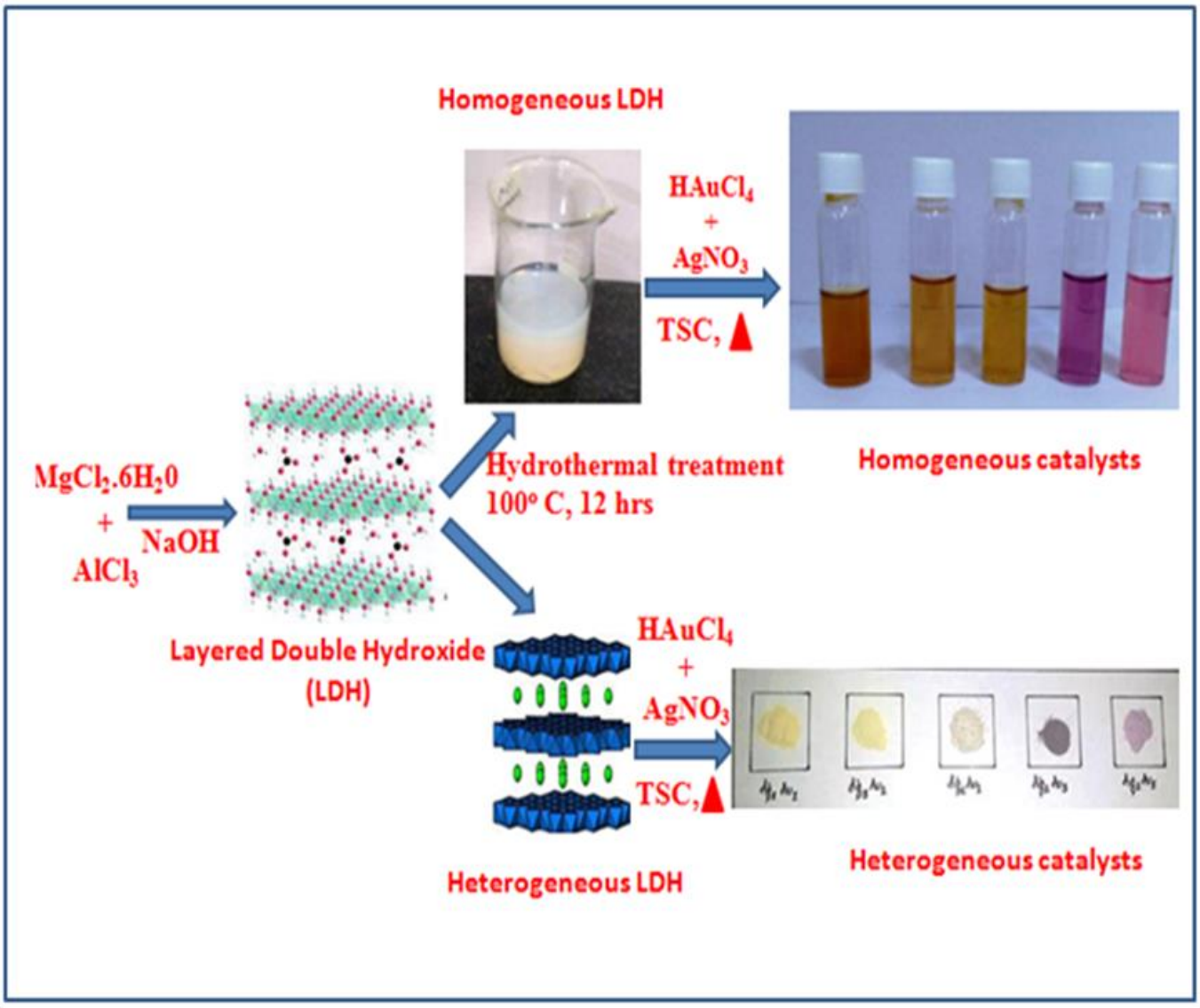

Scheme 2: The schematic representation of the synthesis of homogeneous as well as heterogeneous catalysts.

The Au@LDH NP's, Ag@LDH NP's and alloyed Ag-Au@LDH catalysts were prepared by co-reduction process. This chapter deals with the resultant change in their surface structural morphology and various physicochemical properties including catalytic activity as investigated by different characterization techniques described below. It also includes the kinetic study performed to see the changes.

4.1 Optical Properties of Au-Ag@LDH NP's

4.1.1 UV-Visible Spectroscopy

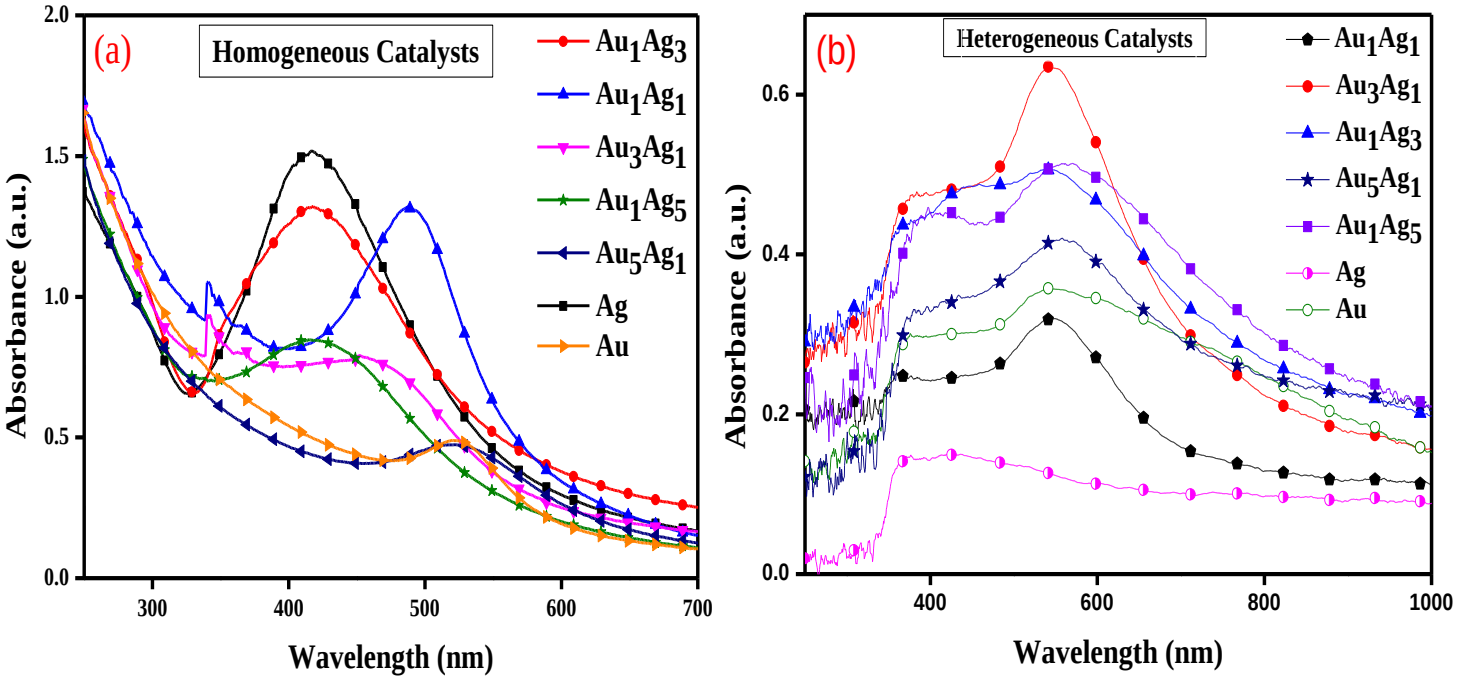

Fig. 11: UV-Visible spectra of different (a) homogenous catalysts and (b) heterogeneous catalysts with different Au-Ag ratio.

The pre-synthesized LDH were used as the seed for the deposition of Au and Ag, to form bimetallic NP's. Besides, the surface plasmon resonance (SPR) effect, metal NP's exhibits the combined oscillation of surface electrons and absorbs the visible light. The absorption band of Au NP's was positioned at 528 nm and that of Ag NP's are positioned at 417 nm [30, 31]. When Ag and Au are mixed together to form an bimetallic alloy NP's, there

is a blue shift from the position of Au and red shift from the position of Ag. This observation is analogues to the formation of Au-Ag bimetallic alloyed structure. For $Au_1Ag_1$the λ_{max} at 489 nm is observed but if the molar ratio of Au increases, the peak is red shifted (for Au_5Ag_1, λ_{max} at 523 nm) whereas with the increase of Ag molar ratio peak is blue shifted (for Au_1Ag_5, λ_{max} at 415 nm) (Fig. 9a). Similar results are seen for heterogeneous catalysts as analysed from DRS (Fig. 9b).

4.2 Structural and Morphological Properties

4.2.1 X-Ray Dispersion (XRD)

The XRD of the synthesized catalyst was done in order to see the composition and planes. Fig. 10 shows the X-Ray analysis of LDH and Ag-Au loaded LDH nanocomposites.

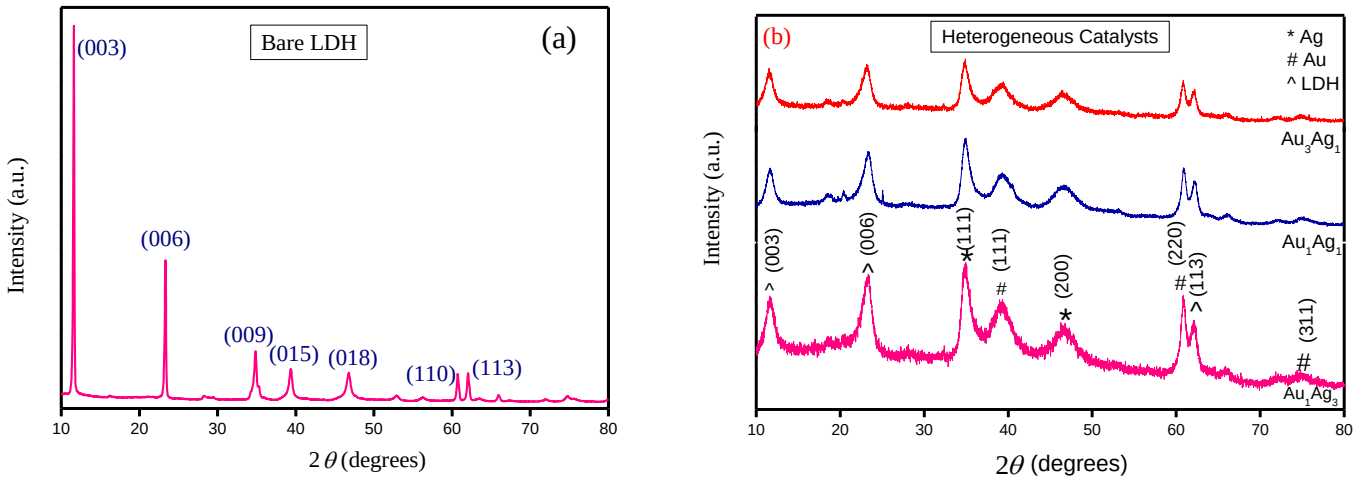

Fig.12: XRD pattern of (a) bare LDH and (b) heterogeneous Au-Ag-LDH supported catalyst.

The reflection pattern of LDH resembles with that of hydrotalcite like layered structured materials having peak positions at 2Θ = 11.60°, 23.34°, 34.81°, 39.45°, 46.64°, 60.82°, 62.34°, 75.14° which correspond to (003) , (006) , (009) , (015) , (018) , (110) and (113) planes (JCPDS No. 01-089-0460, Fig. 10 (a). But after incorporating bimetallic Ag-Au nanoparticles on LDH, broad reflection peaks were observed for both Au and Ag NP's resulting in nanocomposites. Peaks related to Au NP's were found at 2Θ=38.15°, 64.67 ° and 76.4 ° indexed to (111) and (220) and (311) planes (JCPDS No.03-065-2870). Similarly, peaks of Ag NP's are positioned at 2Θ= 35.88° and 47.31°, related to (111) and (200) planes

(JCPDS No. 01-087-0598). The crystallite size of Au and Ag NP's was calculated using Debye-Scherrer equation 0.9 λ/βcosΘ. The crystallite size of Au NP's was found to be 2.26 nm and that of Ag NP's 11.1 nm.

4.2.2 Dynamic Light Scattering

4.2.2.1 Zeta Potential (ζ)

When NP's are dispersed in an aqueous solution, there is adsorption or surface ionization of cations or anions, which results in the formation of electrical double layer leading to the development of new surface charge measured by Zeta potential (ζ). DLS was also done to analyse the zeta potential developed as a result of electrical double layer formed at the particle surface and support. The value of the zeta potential indicates the probable behaviour of the dispersion. Particles which have zeta potential between – 30mV to +30 mV shows the tendency to the coagulate [32]. Since the values for as synthesized homogeneous catalysts are greater than -30 mV (Table-3) so the particles are well dispersed and are stable in the homogeneous medium.

Table 3: Summary of Zeta potential of homogeneous catalysts.

Sample Name	Zeta Potential (mV)
Ag_1Au_1	-31.4
Ag_1Au_3	-30.8
Ag_3Au_1	-31.9
Ag_1Au_5	-38.1
Ag_5Au_1	-41.1
Au	-39.5
Ag	-35.3

4.2.2.2 Particle Size Distribution

The addition of second metal to first may lead to the change in the particle size of bare NP's. Therefore, the measurement of hydrodynamic size distribution of different BM NP's dispersed in water was carried out where; the samples were lighted with 635 nm solid state laser ranged between 15 to 150 mW. The scattered light was detected at an angle of 90◦ with an avalanche photodiode detector.

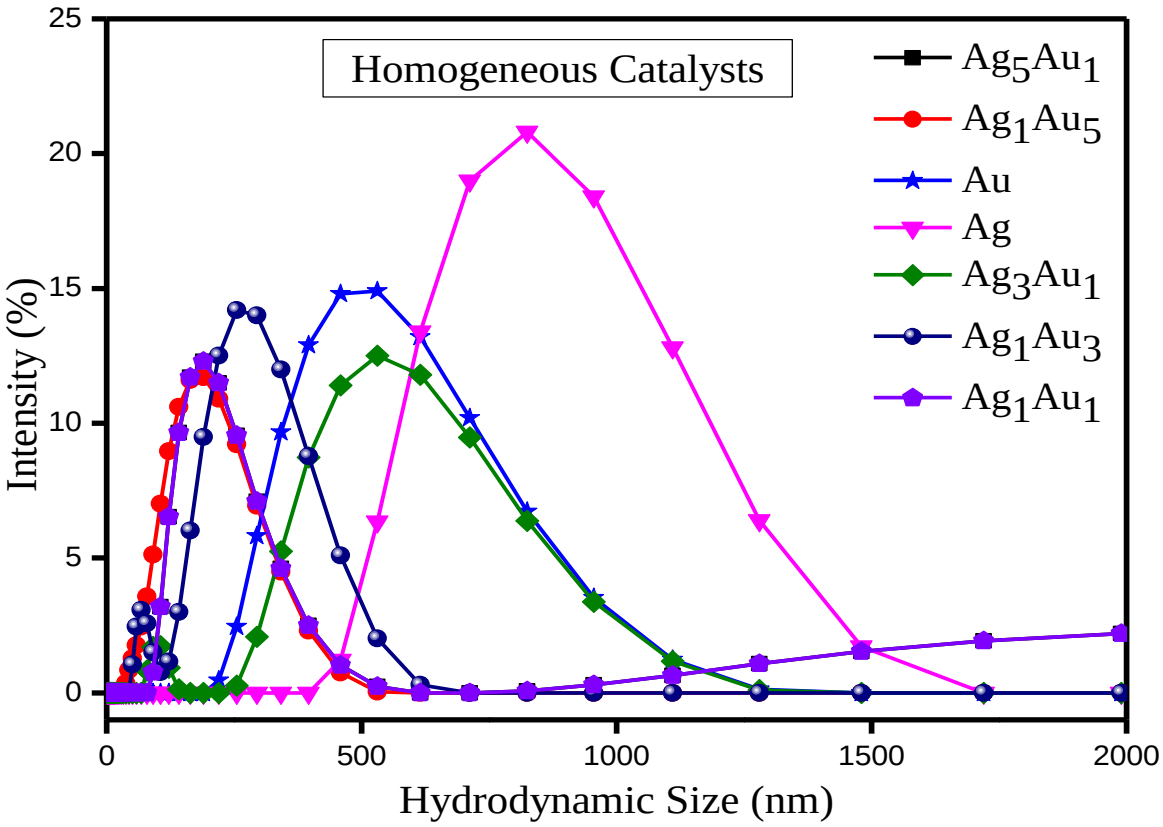

Fig. 13: The figure shows the DLS particle size distribution curves for the homogeneous samples.

It was seen that the average hydrodynamic diameter of Au-Ag@LDH alloyed NP's, upon addition of Au^{+} to the Ag^{+} exhibited decrease in particle diameter signifying the successful formation of alloyed NP's. The hydrodynamic size was found to be highest for Ag (824 nm). As the amount of Au added is increased, the hydrodynamic size goes on decreasing and is found to be lowest for Au_5Ag_1 (184 nm). The observed hydrodynamic diameter was found to be greater than the TEM size due to the adherence of the hydration layer on the NP's surface while estimating the size by DLS. The NP's in liquid undergoes a random Brownian motion which fluctuate the scattered light of the DLS with respect to time intensity.

4.3 Transmission Electron Microscopy

Transmission electron microscope is one of the influential techniques to examine the particle size of metal NP's on catalytic support. The Au-Ag bimetallic NP's supported by LDH was found to be spherical in shape and uniformly dispersed (Fig. 12). The spherical particles are observed due to charge separation and distribute evenly on the surface of a spherical particle (uniformity of electron density on the surface). The addition of Ag and Au together in the presence of trisodium citrate leads to homogenous mixture of alloy NP's (Fig. 12) and give rise to formation of alloyed structure of NP's. The mean diameter of Au-Ag NP's is found to be 50-60 nm for heterogeneous catalyst (Fig. 12b) and 40-50 nm for homogeneous catalyst (Fig. 12a). Fig. 12(d) shows the size distribution of the catalyst which was calculated manually by taking into deliberation the mean of 15–20 particles from the TEM image.

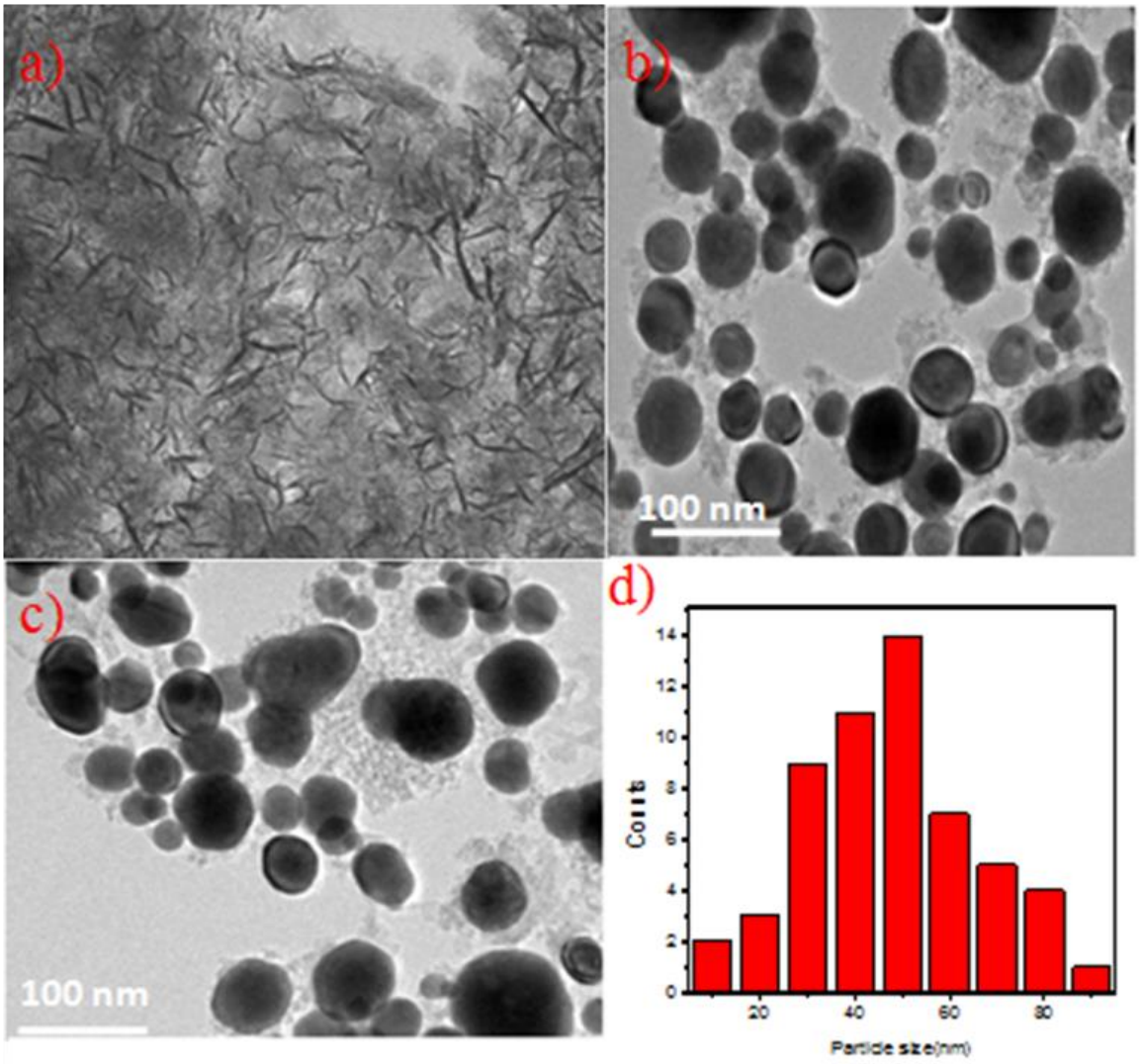

Fig. 14: TEM images of (a) LDH (b) homogeneous Au_1Ag_1catalyst (c) heterogeneous Au_1Ag_1catalyst and (d) particle size distribution chart.

4.4 Scanning Electron Microscope

SEM analysis was performed to gain information about the particle morphologies.

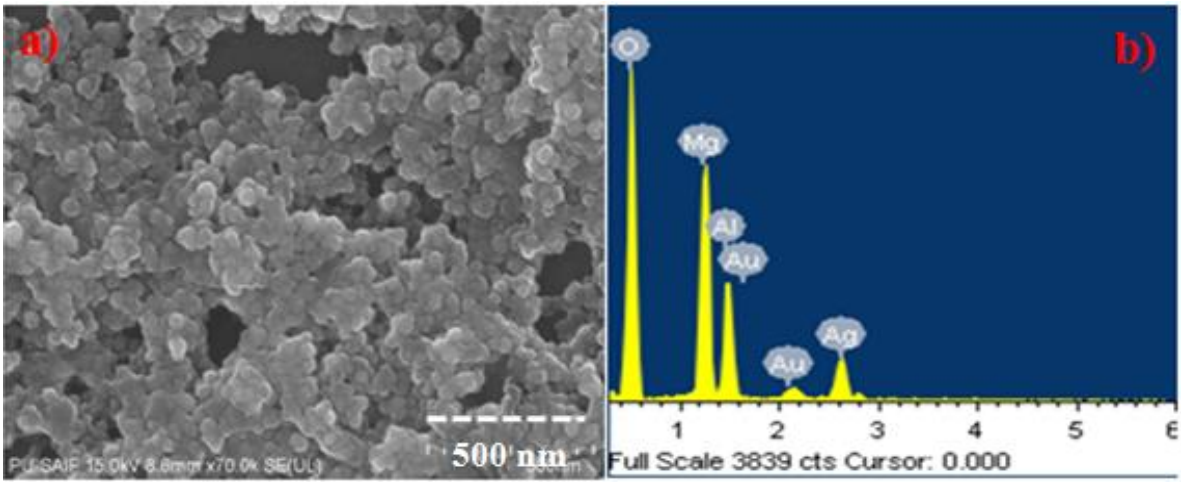

Fig. 15: (a) SEM micrographs (b) EDS pattern of Au_1Ag_1 LDH supported catalyst.

Further, EDS with elemental mapping was used to confirm the bimetallic structure and the distribution of Au/Ag nanoparticles (Fig. 14). Fig. 14 shows that the atoms of Au and Ag have a homogeneous distribution pattern. Analysing the mapping of the sample, the Ag and Au NP's were positioned at the same place showing the formation of bimetallic structure. Also, the disoriented distribution shows the formation of alloy where the silver and gold particles are randomly distributed.

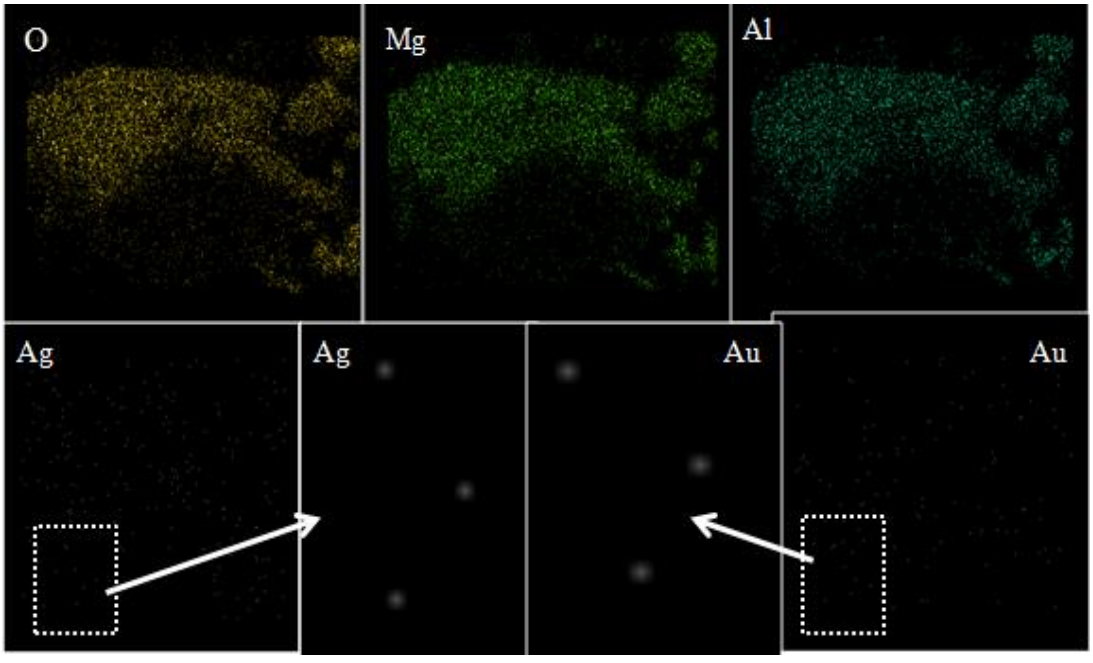

Fig. 16: Colour Mapping of Au_1Ag_1 LDH supported catalyst.

Energy Dispersive X-ray (EDS) Spectroscopy was used for the elemental analysis or chemical composition of the selected points or areas of the sample qualitatively and semi-quantitatively. This technique was used as an attachment on scanning electron microscopy (SEM) or transmission electron microscopy (TEM) and utilizes the high-energy e- that are ejected by an elastic collision of an incident e- with sample's atom nucleus and are referred to as backscattered e-. The yield of backscattered is in proportional to the atomic number of an element and therefore, the sample composition, elements and compounds, and their relative ratios in the area of one micrometre in diameter are determined using this technique. This EDX analysis was carried on JEOL JSM-6510LB.

4.5 X-Ray Photoelectron Spectroscopy (XPS) Analysis

The XPS spectrum shows peaks corresponding to aluminium, magnesium, oxygen, gold and silver (Fig. 15). Aluminium, magnesium and oxygen were the main elements found in LDH structure. The spectrum of gold shows binding energy of Au $4f_{7/2}$ at 84.0 and Au $4f_{5/2}$ at 87.7 eV, which are different from Au^{+} $4f_{7/2}$ (84.6 eV) and Au^{3+} $4f_{7/2}$ (87.0 eV) [33].

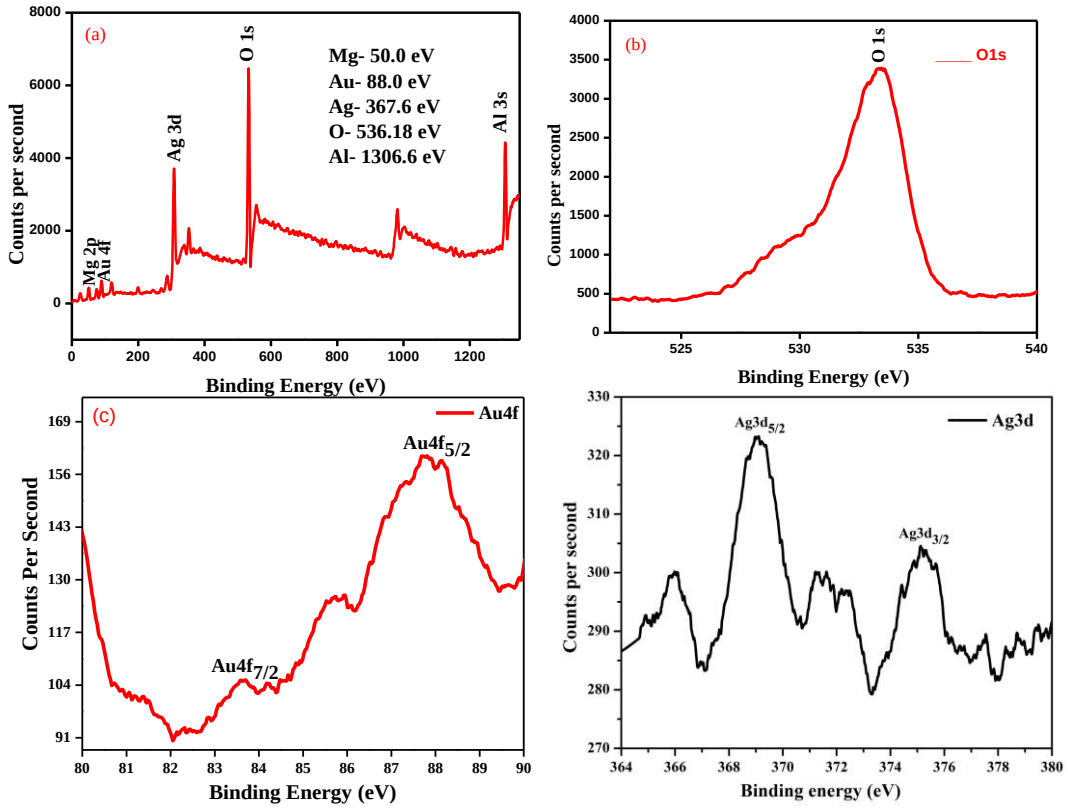

Fig. 17: XPS spectra of (a) Au_1Ag_1 LDH supported catalyst (b) Oxygen (c) Gold (d) Silver.

This suggests that the gold species are in the elemental state and these binding energy values correspond to the metallic gold particles. The spectrum of Ag shows the binding energy of Ag $3d_{5/2}$ at 369 eV and that of Ag $3d_{3/2}$ at 365.8 eV which confirms the elemental state of Ag as well [34]. These results further confirm that the Au and Ag NP's on the surface of LDH support are in zero valence state.

4.6 Nitrogen Sorption Analysis (BET)

Table-4presents theN_2 adsorption/desorption isotherms for Au-Ag catalysts, which reveal their important structural characters. All the catalysts showed adsorption type-IV isotherm with H1 type hysteresis loop on relative pressure (p/p_0 = 0.5-0.9), which indicates the uniform filling of the pores (Fig. 16). The surface area is found to be highest (71.4 m^2/gm) for Au_3Ag_1 heterogeneous catalyst which results the best reduction of 4-NP. Pore size distribution curves which are obtained from desorption branch of nitrogen isotherm via BJH (Barrett-Joyner-Halenda) method are summarized in Table-2.It can be observed that the host LDH has a mean pore diameter of ~ 23 nm and surface area of 35.4 m^2/gm. But upon loading of bimetallic NP's the surface area increases as well as pore diameter decreases.

Table 4: Summary of BET analysis of homogeneous and heterogeneous catalysts.

Sample Name	Surface Area (m^2/gm)	Total Pore Volume(cm^3/g)	Mean Pore Diameter (nm)
Au_1Ag_1	37.6	0.082	8.72
Au_3Ag_1	71.4	0.15	8.47
Au_1Ag_3	26.3	0.063	10.23
Au_5Ag_1	56.61	0.940	8.56
Au_1Ag_5	21.4	0.042	10.89
Ag	38.61	0.125	8.86
Au	46.3	0.10	7.50
LDH	40.55	0.209	22.44

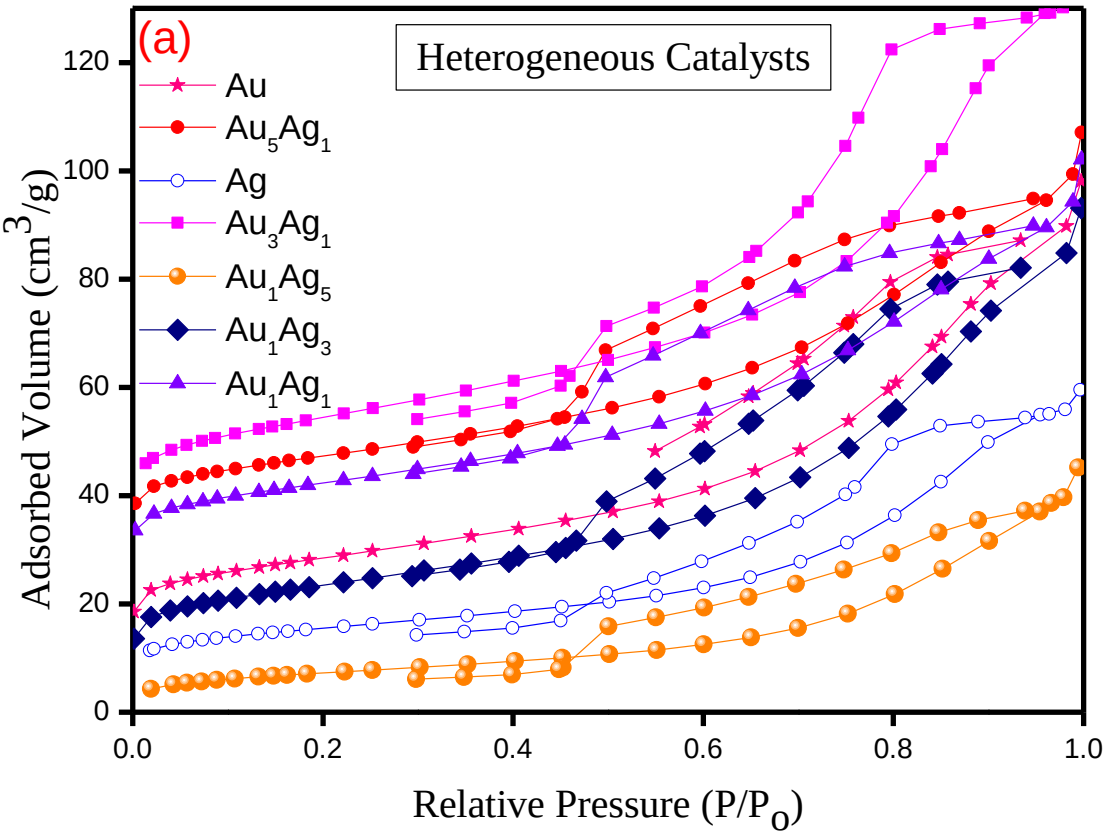

Fig. 18: **BET curves of the various heterogeneous samples with different Au-Ag ratio.**

4.7 Catalytic Reduction of 4-Nitrophenol

The kinetics of 4-NP reduction in presence of bimetallic NP's was studies by using UV-Vis spectroscopy. Since the concentration of bimetallic NP's in the system is quite low, the measurement of absorption spectra of 4-NP and reaction product of 4-AP was not disturbed by the light scattering due to the catalyst carrier particles in the solution. The successive decrease of peak intensity at 400 nm can be attributed to determine the rate constant (Fig. 17). The peak at 400 nm is due to the intermediate formed i.e. nitrophenolate ion in the course of reaction [35]. Aqueous solution of 4-NP shows absorption peak at 317 nm [36]. When the freshly prepared reducing agent ($NaBH_4$) is added the peak is shifted to 400 nm showing the formation of nitrophenolate ion. This peak formed remains constant with time and does not alter in the course of reaction which suggests that the reduction does not proceed without catalyst. After the gradual addition of catalyst, the peak at 400 nm decreases with time.

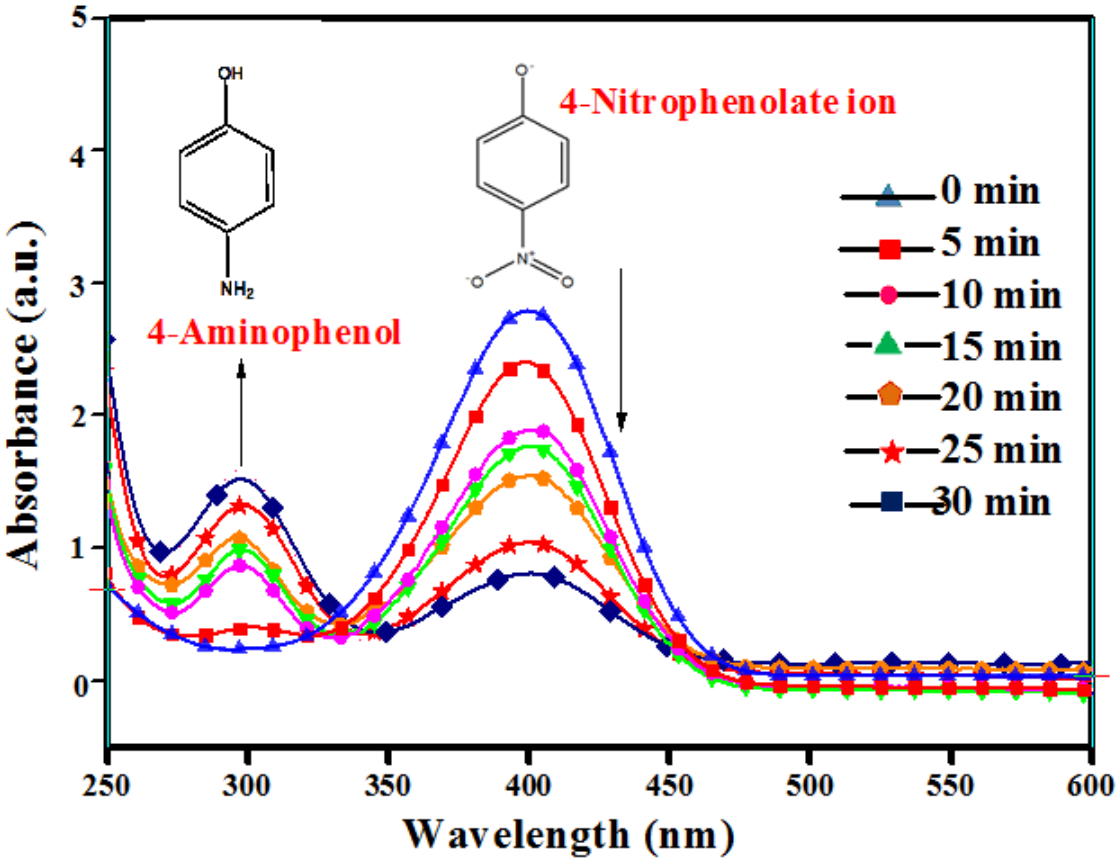

Fig. 19: UV-Visible spectra for the catalytic reduction of 4-NP using $NaBH_4$ in presence of Au_3Ag_1- LDH supported homogeneous catalyst.

As this stage peak at 400 nm decreases and an increase in the peak at 295 nm is seen due to formation of 4-AP [37]. Moreover, a single point of intersection could be observed in the UV-Vis spectra, where all the spectra intersect. This indicates that in the catalytic reduction the conversion of 4-NP gives only product 4-AP [35]. The linear relationship between normalized concentration (C/Co) and reaction time gives the rate of conversion of 4-NP to 4-AP.Since the concentration of reducing agent i.e. sodium borohydride largely exceeds the concentration of 4-NP, the reduction rate can be assumed to be independent of borohydride concentration. So, the reaction is assumed to follow pseudo first order kinetics [38].

All the catalyst synthesized both homogeneous and heterogeneous were used to check the conversion of 4-NP to 4-AP. All the homogeneous catalysts perform well (with respect to rate of reaction) than heterogeneous catalyst as evident from the kinetic rate graph. Fig. 18(a) shows ln (C_t/C_o) vs. T plot for heterogeneous samples and Fig. 18(b) shows ln (C_t/C_o) vs. T plot for homogenous samples. Observing the plot of ln (C_t/C_o) vs. time, it can be seen that

there is a linear relation between these two. The rate constant is calculated from the slope of line. Out of all the catalysts, Au_3Ag_1 (for both homo- and heterogeneous catalyst) shows the best activity which may be due to its greater surface area as seen from BET analysis. On comparing the rate of reaction for homogeneous and heterogeneous catalysts, the rate of reduction of nitro-phenol was greater in case in homogenous catalyst as compared to heterogeneous because in homogenous all the reactants and catalyst are in the same phase, so the interaction is quite easy whereas in case of heterogeneous catalyst, the catalyst and reactants are in different phases due to which interaction is slow.

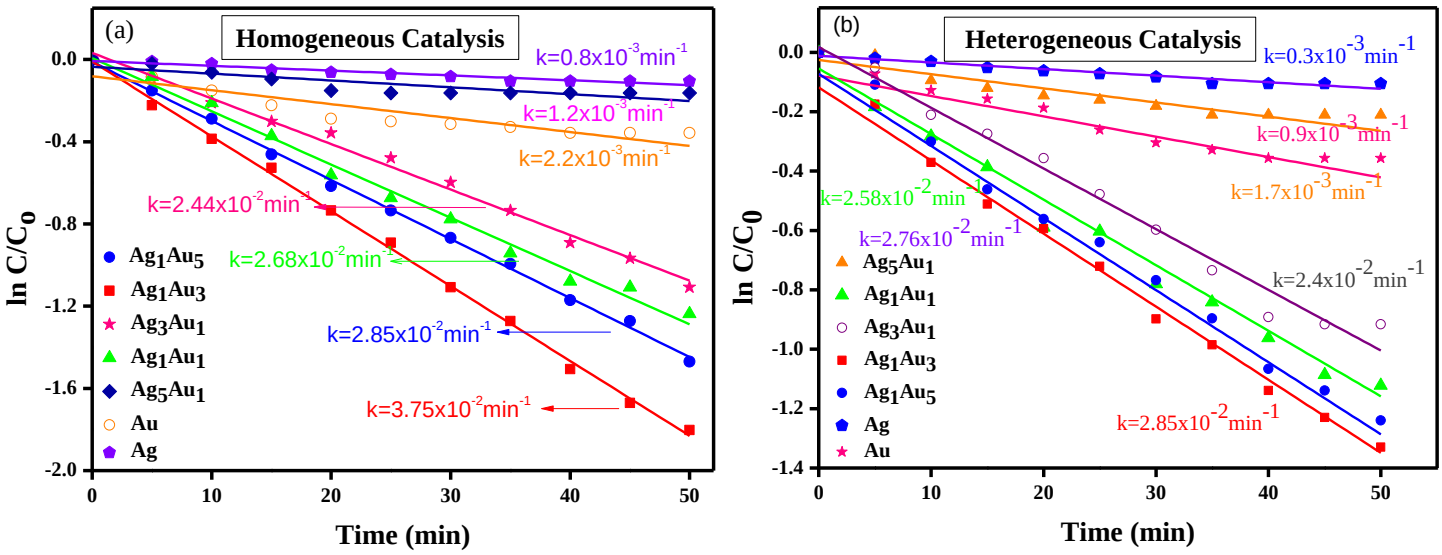

Fig. 20: Plot of ln(C/C₀) vs. time of different (a) homogenous catalysts and (b) heterogeneous catalysts.

Here, attention must be paid to the fact that a delay time t_o was found for the catalytic reduction in all the cases, which may be due to an activation of the catalyst in the reaction mixtures. This is in accord with other studies of the catalysis of this reaction by metal nanoparticles [39-43]. Moreover, a delay in time t_o was found for the catalytic reductions, which were made under air. A similar observation has been noticed by other groups also [44]. Ballauff *et al.* has investigated that this delay in time was attributed to the presence of oxygen present in the system [45]. After the adding of $NaBH_4$, the metal particles start the catalytic reduction by relaying electrons from the donor BH_4^- (donor) to the acceptor 4-NP right after the adsorption of both onto the catalyst particle surface. The excess $NaBH_4$ used, increases the pH of the reaction medium and thus retard the degradation of borohydride ions. The reduction of oxygen proceeds much faster than the nitro-phenols present in the system. The reduction reaction of 4-NP only starts after all the oxygen in the system has reacted. Therefore, the aerial oxidation of 4-AP was prevented. Again, evolution of small bubbles of

the hydrogen gas surrounding the catalyst particles remain well distributed in the reaction mixture during the course of the reaction and offer a favourable condition for a smooth reaction to occur. As $NaBH_4$ is present in large excess, its consumption for the reduction of oxygen did not alter its concentration notably. Induction period observed at the initial stages of the reaction becomes shorter as the particle size decreases [46].

4.8 Kinetic Study

4.8.1 Effect of Catalyst Amount

After the reaction was done, the amount of catalyst was varied to probe its effect on the reaction. Fig. 19(a) shows the plot of rate of reaction vs. amount of catalyst for homogeneous catalyst. As expected and seen, the rate of reaction gradually increases with the increase in the amount of catalyst. The reduction starts to take place at a faster rate and follows a linear relationship. A similar kind of result is seen in case of heterogeneous catalyst shown in Fig. 19(b). It was found that on increasing the amount of catalyst, the rate of reaction increases linearly for both the homogeneous as well as heterogeneous catalyst.

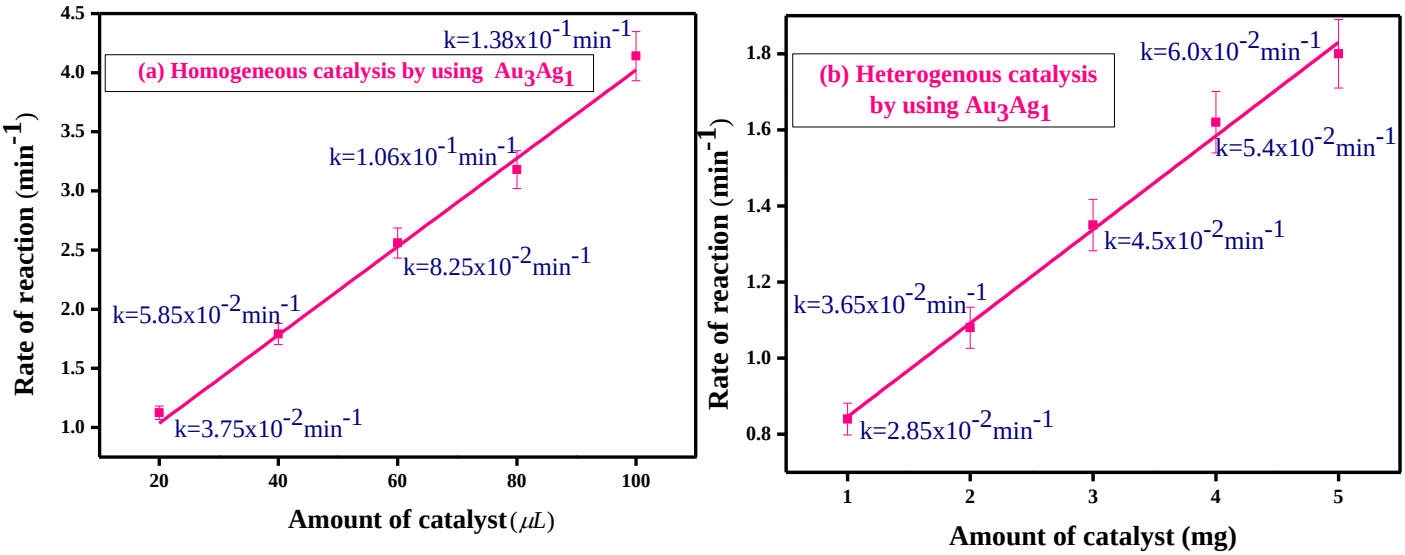

Fig. 21: Effect of catalyst concentration on rate of reaction using (a) Au_3Ag_1-LDH supported homogenous catalyst and (b) Au_3Ag_1-LDH supported heterogeneous catalyst.

4.8.2 Effect of $NaBH_4$ Amount

After seeing the effect of catalyst on rate of reaction, the reaction was performed by varying the amount of reducing agent to probe its effect on the reaction. The plot of rate of reaction vs. amount of $NaBH_4$ is shown in Fig. 20(a) for homogeneous catalysts. As observed, the rate of reaction gradually increases with an increase in the amount of reducing agent. The reduction starts to take place at a faster rate and follows a linear relationship initially but after certain amount of $NaBH_4$, it saturates and the rate of reaction is almost constant. This is because with increase in reducing agent, the amount of electrons required by 4-NP remains same and hence after certain addition there is no effect on the rate of reaction. A similar kind of result is observed in case of heterogeneous catalyst shown in Fig. 20(b). It was found that on increasing the amount of reducing agent, the rate of reaction increases linearly initially but then becomes constant for both the homogeneous as well as heterogeneous catalyst.

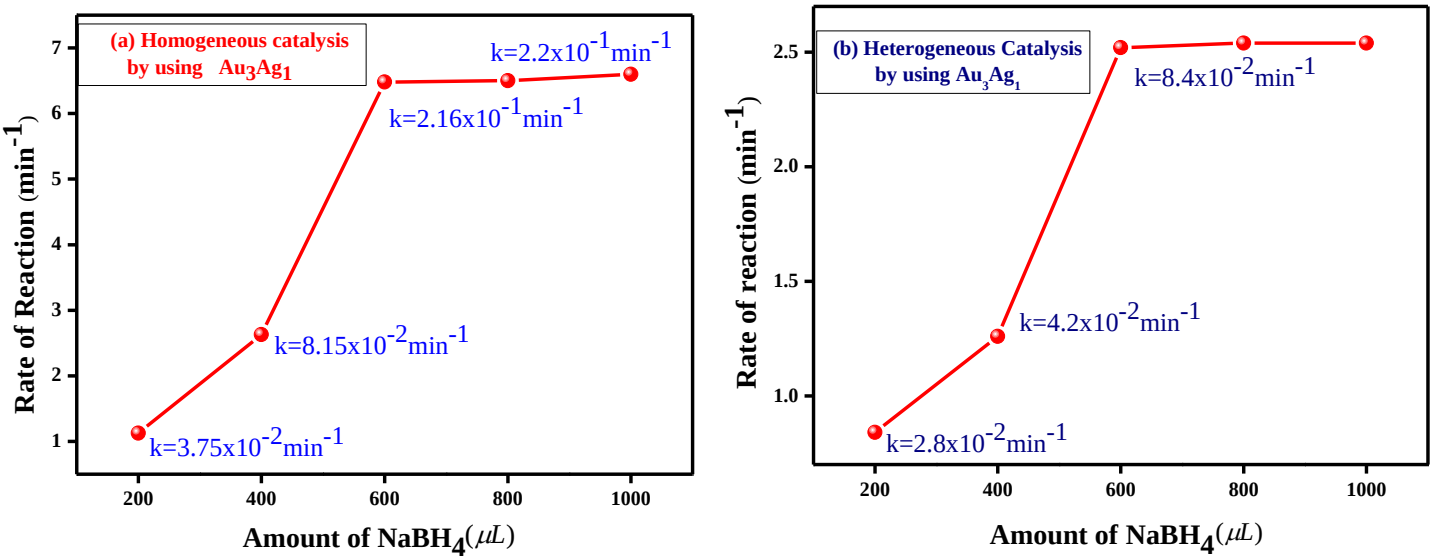

Fig. 22: Effect of $NaBH_4$ concentration on rate of reaction using (a) Au_3Ag_1-LDH supported homogenous catalyst and (b) Au_3Ag_1-LDH supported heterogeneous catalyst.

4.8.3 Effect of Amount of 4-NP

The reaction was also performed by varying the amount of NP to probe its effect on the reaction. The plot of rate of reaction vs. amount of NP is demonstrated in Fig. 21(a) for homogeneous catalyst. As observed, the rate constant gradually remains constant with an increase in the amount of reducing agent. The rate of reaction is given by the equation:

$$\text{Rate} = k\,(\text{reactant})^1$$

Following this equation, the rate of reaction increases with the increase in the amount of 4-NP. A similar kind of result is seen in case of heterogeneous catalyst which is shown in Fig. 21 (b). It was found that on increasing the amount of 4-NP, the rate of reaction increases linearly initially but then becomes constant for both the homogeneous as well as heterogeneous catalyst.

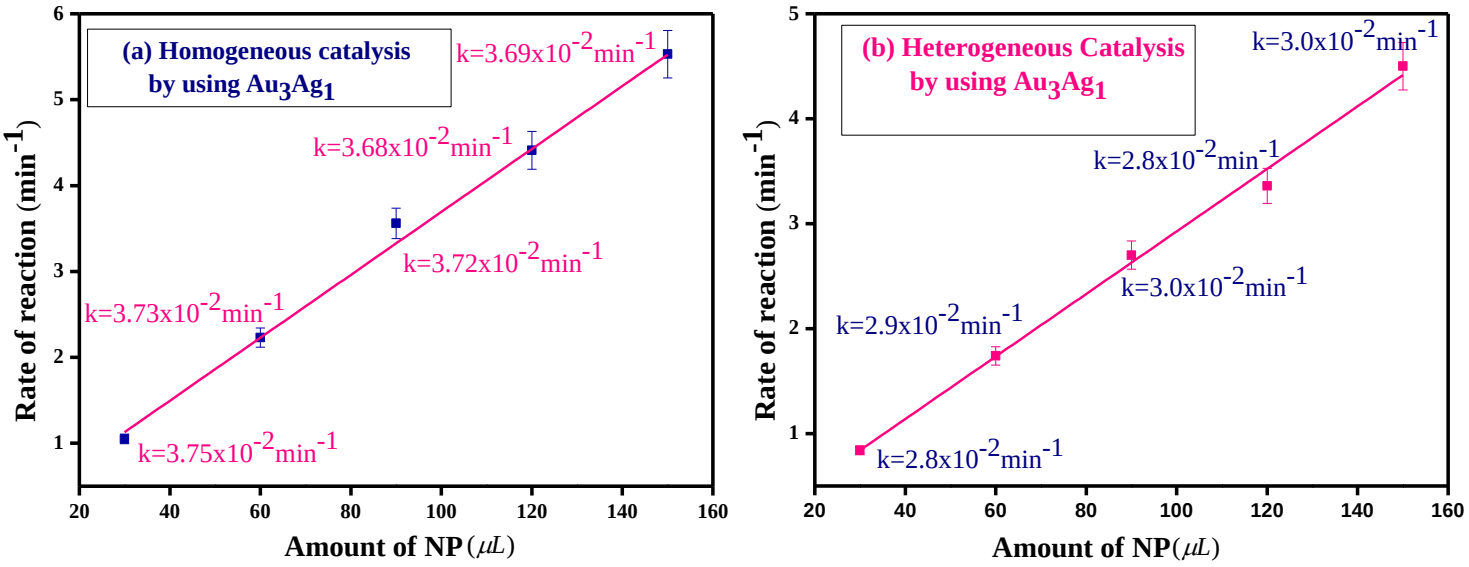

Fig. 23: Effect of concentration of NP on rate of reaction using (a) Au_3Ag_1-LDH supported homogeneous catalyst and (b) Au_3Ag_1-LDHsupported heterogeneous catalyst.

4.9 Reusability

Though the homogeneous catalysts are known for their high selectivity and conversion, heterogeneous catalyst are known for their reusability. The catalyst used to performed the catalytic reduction was washed and dried and then was made to again catalyze the reduction. The graph for reusability of the heterogeneous catalyst is shown in Fig. 22. It was seen that the same catalyst could be used at least for 5 times with 93% efficiency. This is essential for industrial applications where the catalyst could be easily recycled and reused with better efficiency.

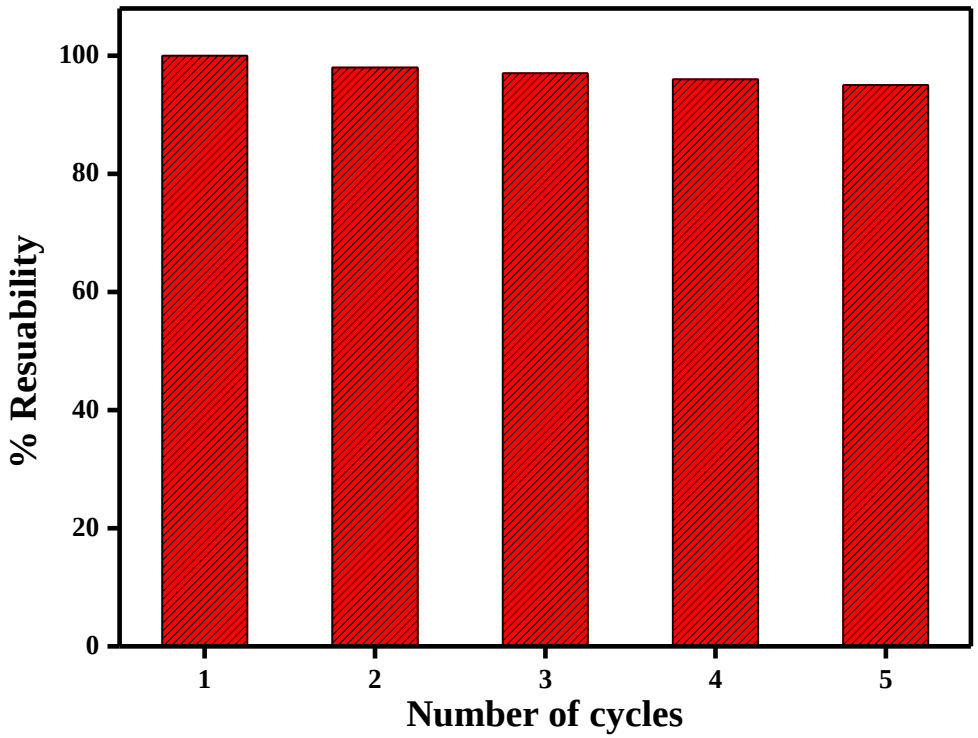

Fig. 24: Reusability graph of Au_3Ag_1 LDH supported heterogeneous catalyst for 4-NP reduction.

CHAPTER 5: CONCLUSION

In the present study, homogeneous and heterogeneous Au-Ag bimetallic NP's was successfully synthesized on LDH support. The average diameter of homogeneous and heterogeneous Au-Ag bimetallic NP's on LDH is 30-50 nm. The highest catalytic activity for homogeneous catalysts may be attributed to the synergistic effect and homogenous dispersion of Au-Ag bimetallic NP's on LDH surface. This is the first fruitful exploitation of its kind where the rate kinetics was studied for both homogeneous and heterogeneous system on the reduction of 4-nitrophenol. The new as-prepared Au-Ag bimetallic NP's supported on LDH are stable, efficient, eco-friendly, easy to prepare, and recyclable and thus have potential for industrial applications.

5.1 Future Prospective

- To study the same reaction with other coinage metals.
- To study reduction of other derivates of NP with the same catalyst.
- To study the effect other supports can have on the reduction reaction.
- To fabricate core@shell NP's of same coinage metals and study the difference in the reduction reaction.

CHAPTER 6: REFERENCES

1. Studt, F., et al., *Identification of non-precious metal alloy catalysts for selective hydrogenation of acetylene.* Science, 2008. **320**(5881): p. 1320-1322.
2. Xiao, C., et al., *Intermetallic NaAu2 as a heterogeneous catalyst for low-temperature CO oxidation.* Journal of the American Chemical Society, 2013. **135**(26): p. 9592-9595.
3. Studt, F., et al., *Discovery of a Ni-Ga catalyst for carbon dioxide reduction to methanol.* Nature chemistry, 2014. **6**(4): p. 320-324.
4. Armbrüster, M., et al., *Al13Fe4 as a low-cost alternative for palladium in heterogeneous hydrogenation.* Nature materials, 2012. **11**(8): p. 690-693.
5. Noguez, C., *Surface plasmons on metal nanoparticles: the influence of shape and physical environment.* The Journal of Physical Chemistry C, 2007. **111**(10): p. 3806-3819.
6. Pyayt, A.L., et al., *Integration of photonic and silver nanowire plasmonic waveguides.* Nature nanotechnology, 2008. **3**(11): p. 660-665.
7. Peng, S., et al., *A facile synthesis of monodisperse Au nanoparticles and their catalysis of CO oxidation.* Nano research, 2008. **1**(3): p. 229-234.
8. Murphy, C.J., et al., *Chemical sensing and imaging with metallic nanorods.* Chemical Communications, 2008(5): p. 544-557.
9. Murphy, C.J., et al., *Gold nanoparticles in biology: beyond toxicity to cellular imaging.* Accounts of chemical research, 2008. **41**(12): p. 1721-1730.
10. Cao, Y.C., R. Jin, and C.A. Mirkin, *Nanoparticles with Raman spectroscopic fingerprints for DNA and RNA detection.* Science, 2002. **297**(5586): p. 1536-1540.
11. Mulvihill, M.J., et al., *Anisotropic etching of silver nanoparticles for plasmonic structures capable of single-particle SERS.* Journal of the American Chemical Society, 2009. **132**(1): p. 268-274.
12. Bastús, N.G., J. Piella, and V. Puntes, *Quantifying the sensitivity of multipolar (dipolar, quadrupolar, and octapolar) surface plasmon resonances in silver nanoparticles: The effect of size, composition, and surface coating.* Langmuir, 2016. **32**(1): p. 290-300.

13. Watanabe, K., et al., *Photochemistry on metal nanoparticles.* Chemical reviews, 2006. **106**(10): p. 4301-4320.
14. Bedioui, F., *Zeolite-encapsulated and clay-intercalated metal porphyrin, phthalocyanine and Schiff-base complexes as models for biomimetic oxidation catalysts: an overview.* Coordination Chemistry Reviews, 1995. **144**: p. 39-68.
15. Czaplinska, J., I. Sobczak, and M. Ziolek, *Bimetallic AgCu/SBA-15 system: the effect of metal loading and treatment of catalyst on surface properties.* The Journal of Physical Chemistry C, 2014. **118**(24): p. 12796-12810.
16. Roucoux, A., J. Schulz, and H. Patin, *Reduced transition metal colloids: a novel family of reusable catalysts?* Chemical reviews, 2002. **102**(10): p. 3757-3778.
17. Xu, Z.P., et al., *Dispersion and size control of layered double hydroxide nanoparticles in aqueous solutions.* The Journal of Physical Chemistry B, 2006. **110**(34): p. 16923-16929.
18. Saha, S., et al., *Photochemical green synthesis of calcium-alginate-stabilized Ag and Au nanoparticles and their catalytic application to 4-nitrophenol reduction.* Langmuir, 2009. **26**(4): p. 2885-2893.
19. Corbett, J.F., *An historical review of the use of dye precursors in the formulation of commercial oxidation hair dyes.* Dyes and Pigments, 1999. **41**(1): p. 127-136.
20. Rode, C., M. Vaidya, and R. Chaudhari, *Synthesis of p-aminophenol by catalytic hydrogenation of nitrobenzene.* Organic process research & development, 1999. **3**(6): p. 465-470.
21. Sharma, M., et al., *Enhanced catalytic and antibacterial activity of nanocasted mesoporous silver monoliths: kinetic and thermodynamic studies.* Journal of Sol-Gel Science and Technology, 2016: p. 1-7.
22. Mehta, A., et al., *Gold Nanoparticles Grafted Mesoporous Silica: A Highly Efficient and Recyclable Heterogeneous Catalyst for Reduction of 4-Nitrophenol.* Nano, 2016. **11**(09): p. 1650104.
23. Wu, T., et al., *Fabrication of graphene oxide decorated with Au–Ag alloy nanoparticles and its superior catalytic performance for the reduction of 4-nitrophenol.* Journal of Materials Chemistry A, 2013. **1**(25): p. 7384-7390.
24. Pozun, Z.D., et al., *A systematic investigation of p-nitrophenol reduction by bimetallic dendrimer encapsulated nanoparticles.* The Journal of Physical Chemistry C, 2013. **117**(15): p. 7598-7604.

25. Zhang, J., et al., *Gold nanoparticle decorated ceria nanotubes with significantly high catalytic activity for the reduction of nitrophenol and mechanism study.* Applied Catalysis B: Environmental, 2013. **132**: p. 107-115.
26. Kästner, C. and A.F. Thünemann, *Catalytic Reduction of 4-Nitrophenol Using Silver Nanoparticles with Adjustable Activity.* Langmuir, 2016. **32**(29): p. 7383-7391.
27. Menumerov, E., R.A. Hughes, and S. Neretina, *The Catalytic Reduction of 4-Nitrophenol: A Quantitative Assessment of the Role of Dissolved Oxygen in Determining the Induction Time.* Nano Letters, 2016.
28. Li, M. and G. Chen, *Revisiting catalytic model reaction p-nitrophenol/NaBH 4 using metallic nanoparticles coated on polymeric spheres.* Nanoscale, 2013. **5**(23): p. 11919-11927.
29. Pandey, S. and S.B. Mishra, *Catalytic reduction of p-nitrophenol by using platinum nanoparticles stabilised by guar gum.* Carbohydrate polymers, 2014. **113**: p. 525-531.
30. dos Santos, D.S., et al., *Gold nanoparticle embedded, self-sustained chitosan films as substrates for surface-enhanced Raman scattering.* Langmuir, 2004. **20**(23): p. 10273-10277.
31. Shameli, K., et al., *Green biosynthesis of silver nanoparticles using Curcuma longa tuber powder.* Int J Nanomed, 2012. **7**(2012): p. 5603-5610.
32. Marsalek, R., *Particle size and zeta potential of ZnO.* APCBEE Procedia, 2014. **9**: p. 13-17.
33. Jiang, P., et al., *PVP-capped twinned gold plates from nanometer to micrometer.* Journal of Nanoparticle Research, 2006. **8**(6): p. 927-934.
34. Lopez-Salido, I., D.C. Lim, and Y.D. Kim, *Ag nanoparticles on highly ordered pyrolytic graphite (HOPG) surfaces studied using STM and XPS.* Surface science, 2005. **588**(1): p. 6-18.
35. Pradhan, N., A. Pal, and T. Pal, *Silver nanoparticle catalyzed reduction of aromatic nitro compounds.* Colloids and Surfaces A: Physicochemical and Engineering Aspects, 2002. **196**(2): p. 247-257.
36. Zhang, Z., et al., *In situ assembly of well-dispersed gold nanoparticles on electrospun silica nanotubes for catalytic reduction of 4-nitrophenol.* Chemical Communications, 2011. **47**(13): p. 3906-3908.
37. Zhang, P., et al., *In situ assembly of well-dispersed Ag nanoparticles (AgNPs) on electrospun carbon nanofibers (CNFs) for catalytic reduction of 4-nitrophenol.* Nanoscale, 2011. **3**(8): p. 3357-3363.

38. Scott, R.W., et al., *Titania-supported PdAu bimetallic catalysts prepared from dendrimer-encapsulated nanoparticle precursors.* Journal of the American Chemical Society, 2005. **127**(5): p. 1380-1381.
39. Mei, Y., et al., *High catalytic activity of platinum nanoparticles immobilized on spherical polyelectrolyte brushes.* Langmuir, 2005. **21**(26): p. 12229-12234.
40. Esumi, K., R. Isono, and T. Yoshimura, *Preparation of PAMAM− and PPI− metal (silver, platinum, and palladium) nanocomposites and their catalytic activities for reduction of 4-nitrophenol.* Langmuir, 2004. **20**(1): p. 237-243.
41. Lu, Y., et al., *Thermosensitive core–shell particles as carriers for Ag nanoparticles: modulating the catalytic activity by a phase transition in networks.* Angewandte Chemie International Edition, 2006. **45**(5): p. 813-816.
42. Praharaj, S., et al., *Immobilization and recovery of Au nanoparticles from anion exchange resin: resin-bound nanoparticle matrix as a catalyst for the reduction of 4-nitrophenol.* Langmuir, 2004. **20**(23): p. 9889-9892.
43. Ghosh, S.K., et al., *Bimetallic Pt–Ni nanoparticles can catalyze reduction of aromatic nitro compounds by sodium borohydride in aqueous solution.* Applied Catalysis A: General, 2004. **268**(1): p. 61-66.
44. Mukherjee, P., et al., *Characterization and catalytic activity of gold nanoparticles synthesized by autoreduction of aqueous chloroaurate ions with fumed silica.* Chemistry of materials, 2002. **14**(4): p. 1678-1684.
45. Sharma, G. and M. Ballauff, *Cationic spherical polyelectrolyte brushes as nanoreactors for the generation of gold particles.* Macromolecular rapid communications, 2004. **25**(4): p. 547-552.
46. Panigrahi, S., et al., *Synthesis and size-selective catalysis by supported gold nanoparticles: study on heterogeneous and homogeneous catalytic process.* The Journal of Physical Chemistry C, 2007. **111**(12): p. 4596-4605.

Nidhi_14-07-2017

ORIGINALITY REPORT

%15	%3	%14	%
SIMILARITY INDEX	INTERNET SOURCES	PUBLICATIONS	STUDENT PAPERS

PRIMARY SOURCES

1	Monga, Anila, and Bonamali Pal. "Improved catalytic activity and surface electro-kinetics of bimetallic Au–Ag core–shell nanocomposites", New Journal of Chemistry, 2014. Publication	%2
2	Kumar, Ashish, Vanama Pavan Kumar, Venkataraman Vishwanathan, and Komandur V.R. Chary. "Synthesis, characterization, and reactivity of Au/MCM-41 catalysts prepared by homogeneous deposition–precipitation (HDP) method for vapor phase oxidation of benzyl alcohol", Materials Research Bulletin, 2015. Publication	%2
3	Mehta, Akansha, Manu Sharma, Ashish Kumar, and Soumen Basu. "Gold Nanoparticles Grafted Mesoporous Silica: A Highly Efficient and Recyclable Heterogeneous Catalyst for Reduction of 4-Nitrophenol", NANO, 2016. Publication	%1
4	Wei, D.. "Chitosan as an active support for assembly of metal nanoparticles and	%1

application of the resultant bioconjugates in catalysis", Carbohydrate Research, 20100111
Publication

---

5 Saha, Sandip, Anjali Pal, Subrata Kundu, Soumen Basu, and Tarasankar Pal. "Photochemical Green Synthesis of Calcium-Alginate-Stabilized Ag and Au Nanoparticles and Their Catalytic Application to 4-Nitrophenol Reduction", Langmuir, 2010.
Publication

%1

---

6 homepage.usask.ca
Internet Source

%1

---

7 Jana, S.. "Synthesis of silver nanoshell-coated cationic polystyrene beads: A solid phase catalyst for the reduction of 4-nitrophenol", Applied Catalysis A, General, 20060925
Publication

%1

---

8 Mehta, Akansha, Amit Mishra, Manisha Sharma, Satnam Singh, and Soumen Basu. "Effect of silica/titania ratio on enhanced photooxidation of industrial hazardous materials by microwave treated mesoporous SBA-15/TiO2 nanocomposites", Journal of Nanoparticle Research, 2016.
Publication

%1

---

9 www.britannica.com
Internet Source

%1

10	Lu, Y.. "'Nano-tree'-type spherical polymer brush particles as templates for metallic nanoparticles", Polymer, 20060628 Publication	%1
11	LIU, S.. "Dodecylsulfate Anion Embedded Layered Double Hydroxide Supported Nanopalladium Catalyst for the Suzuki Reaction", Chinese Journal of Catalysis, 2010 Publication	%1
12	Wu, Tao, Lei Zhang, Jianping Gao, Yu Liu, Chunjuan Gao, and Jing Yan. "Fabrication of graphene oxide decorated with Au–Ag alloy nanoparticles and its superior catalytic performance for the reduction of 4-nitrophenol", Journal of Materials Chemistry A, 2013. Publication	%1
13	Czaplinska, Joanna, Izabela Sobczak, and Maria Ziolek. "Bimetallic AgCu/SBA-15 System: The Effect of Metal Loading and Treatment of Catalyst on Surface Properties", The Journal of Physical Chemistry C, 2014. Publication	%1
14	Lu, Yan, Yu Mei, Matthias Ballauff, and Markus Drechsler. "Thermosensitive Core−Shell Particles as Carrier Systems for Metallic Nanoparticles", The Journal of Physical	%1

Chemistry B, 2006.
Publication

15 Liu, Yan, Lili Liu, Min Yuan, and Rong Guo. "Preparation and characterization of casein-stabilized gold nanoparticles for catalytic applications", Colloids and Surfaces A Physicochemical and Engineering Aspects, 2013. %1
Publication

EXCLUDE QUOTES	ON	EXCLUDE MATCHES	< 1%
EXCLUDE BIBLIOGRAPHY	ON		